Gondwana Research 37 (2016) 39–52

Contents lists available at ScienceDirect

Gondwana Research

journal homepage: www.elsevier.com/locate/gr

Detrital zircons from Neoproterozoic sedimentary rocks in the Yili Block: Constraints on the affinity of microcontinents in the southern Central Asian Orogenic Belt

Zongying Huang [a,b], Xiaoping Long [c,*], Chao Yuan [a], Min Sun [d], Yujing Wang [e], Yunying Zhang [a], Bei Chen [a]

[a] State Key Laboratory of Isotope Geochemistry, Guangzhou Institute of Geochemistry, Chinese Academy of Sciences, Guangzhou 510640, China
[b] University of Chinese Academy of Sciences, Beijing 10069, China
[c] State Key Laboratory of Continental Dynamics, Department of Geology, Northwest University, Northern Taibai Street 229, Xi'an 710069, China
[d] Department of Earth Sciences, The University of Hong Kong, Pokfulam Road, Hong Kong, China
[e] College of Urban and Environmental Science, Northwest University, Northern Taibai Street 229, Xi'an 710069, China

ARTICLE INFO

Article history:
Received 30 August 2015
Received in revised form 5 May 2016
Accepted 6 May 2016
Available online 23 June 2016

Handling Editor: M. Santosh

Keywords:
Yili Block
Detrital zircon
Crustal growth
Tectonic affinity
Central Asian Orogenic Belt

ABSTRACT

The Yili Block is one of the Precambrian microcontinents dispersed in the Central Asian Orogenic Belt (CAOB). Detrital zircon U–Pb ages and Hf isotopic data of Neoproterozoic meta-sedimentary rocks (the Wenquan Group) are presented to constrain the tectonic affinity and early history of the Yili Block. The dating of detrital zircons indicates that both the lower and upper Wenquan Groups have two major populations with ages at 950–880 Ma and 1600–1370 Ma. Moreover, the upper Wenquan Group has two minor populations at ~1100 Ma and 1850–1720 Ma. According to the youngest age peaks of meta-sedimentary rocks and the ages of related granitoids, the lower Wenquan Group is considered to have been deposited during the early Neoproterozoic (900–845 Ma), whereas the upper Wenquan Group was deposited at 880–857 Ma. The zircon $\varepsilon_{Hf}(t)$ values suggest that the 1.85–1.72 Ga source rocks for the upper Wenquan Group were dominated by juvenile crustal material, whereas those for the lower Wenquan Group involved more ancient crustal material. For the 1.60–1.37 Ga source rocks, however, juvenile material was a significant input into both the upper and lower Wenquan Groups. Therefore, two synchronous crustal growth and reworking events were identified in the northern Yili Block at ca. 1.8–1.7 Ga and 1.6–1.3 Ga, respectively. After the last growth and reworking event, continuous crustal reworking took place in the northern Yili Block until the early Neoproterozoic. Comparing the age patterns and Hf isotopic compositions of detrital zircons from the Yili Block and the surrounding tectonic units indicates that the Yili Block has a close tectonic affinity to the Chinese Central Tianshan Block in the Precambrian. The Precambrian crustal evolution of the Yili Block is distinct from that of the Siberian, North China and Tarim Cratons. Such difference therefore suggests that the Yili Block and the Chinese Central Tianshan Block may have been united in an isolated Precambrian microcontinent within the CAOB rather than representing two different blocks rifted from old cratons on both sides of the Paleo-Asian Ocean.

1. Introduction

The Central Asian Orogenic Belt (CAOB) is located between the Siberian, the North China and Tarim Cratons (Fig. 1 inset). The CAOB is a complex collage of ancient microcontinents, island arcs, seamounts and oceanic plateaux (Sengör and Natal'in, 1996; Jahn et al., 2000, 2004; Xiao et al., 2004; Windley et al., 2007; Eizenhöfer et al., 2014; Han et al., 2015; Eizenhöfer et al., 2015a,b; Han et al., 2016a,b). Microcontinents and continental fragments are considered to have been incorporated into the CAOB during its accretion (Windley et al., 2007; Gao et al., 2011; Kröner et al., 2012; Alexeiev et al., 2015; Zhang et al., 2015a,b,c, 2016). However, their origins are still controversial, with some researchers assuming that some microcontinents within the CAOB had a Gondwana derivation and were then accreted onto the southern margin of the Siberian Craton (Zonenshain et al., 1990; Buslov et al., 2001; Dobretsov et al., 2003; Kheraskova et al., 2003; Laurent-Charvet et al., 2003; Xiao et al., 2010). In contrast, models that favor the origin of the Siberian Craton have been proposed recently (Berzin and Dobretsov, 1994; Sengör and Natal'in, 1996; Kuzmichev et al., 2001; Turkina et al., 2007; Zhou et al., 2009, 2010a,b,c, 2011). More recently, the Tarim Craton was also considered to be a possible origin for these microcontinents (Levashova et al., 2009; Lei et al., 2011; Levashova et al., 2011; Rojas-Agramonte et al., 2011; Shu et al., 2011; Ma et al., 2012a,b; Lei et al., 2013; Ma et al., 2013; Liu et al.,

* Corresponding author. Tel.: +86 29 8830 2456.
E-mail address: longxp@nwu.edu.cn (X. Long).

http://dx.doi.org/10.1016/j.gr.2016.05.009
1342-937X/

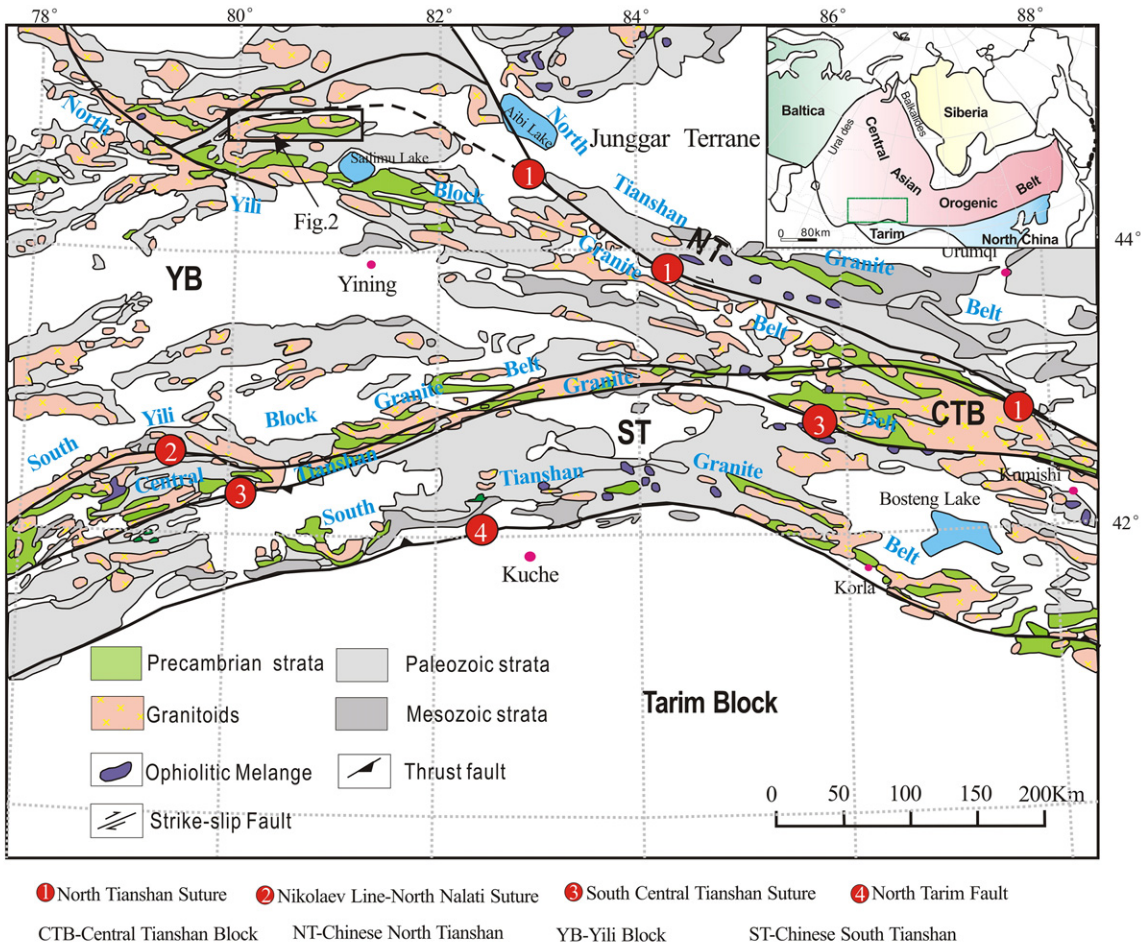

Fig. 1. Simplified geological map of the Chinese Tianshan. Modified after Xiao et al. (2004) and Gao et al. (2009). Inset is a simplified map of the Central Asian Orogenic Belt. Modified after Xiao et al. (2010).

2014; Wang et al., 2014c). These controversies largely result from the Phanerozoic reworking of polyphase orogenesis and magmatism which overprinted and obscured much of the Precambrian geological records.

The Yili Block (YB) is a representative microcontinent with Precambrian basement in the southern CAOB (Fig. 1) (Gao et al., 1998; Shu et al., 2004; Gao et al., 2009; Xiao et al., 2010; Shu et al., 2011). It is located within the Chinese E–W-trending Tianshan orogenic belt surrounding by the Kazakhstan–Kyrgyzstan Tianshan, the Junggar Basin and the Tarim Craton (Fig. 1). Thus, the Yili Block is a key to constrain the origin of microcontinents dispersed within the CAOB. Previous studies have constrained the Paleozoic accretionary process and crustal growth in the Yili Block (Hu et al., 2008; Wang et al., 2008; Tang et al., 2010; Wang et al., 2012; Zhang et al., 2012a; Huang et al., 2013), but the Precambrian evolution is poorly understood. In the Yili Block, most Neoproterozoic rocks were incorrectly assigned to be Paleoproterozoic in age (XBGMR, 1993). Although some magmatic rocks in the Yili Block were found with ages at 926 Ma and 776 Ma (Chen et al., 1999b; Hu et al., 2010; Wang et al., 2014a,b), it remains uncertain whether a Paleoproterozoic to Mesoproterozoic basement exists in this block. This is because (1) Precambrian rocks are sporadically exposed on the surface of the Yili Block; (2) the records of the early geological evolution are obscured by Paleozoic overprinting; and (3) the U–Pb age patterns of detrital and xenocrystic/inherited zircons from various rocks with different ages are very complicated. Therefore, the tectonic affinity, Precambrian crustal growth and reworking of the Yili Block are still uncertain. The key questions concerning the evolution of the Yili Block include: (1) When did the earliest crustal basement rocks form? (2) When did Precambrian crustal growth and reworking happen? (3) Does the block have a tectonic affinity with the Chinese Central Tianshan Block, the Siberian Craton, the North China Craton or the Tarim Craton?

We present U–Pb ages and Hf isotopic data for detrital zircons from Neoproterozoic meta-sedimentary rocks exposed in the northern Yili Block. These data, in combination with regional Precambrian geological records, provide new constraints on formation of the basement and crustal growth and reworking of the Yili Block, which not only illuminate its tectonic affinity and but also shed light on the origin of Precambrian continental terranes within the CAOB.

2. Geological background

The Tianshan Orogen extends for ca. 2500 km from Uzbekistan in the west to Xinjiang Uygur Autonomous Region of northwestern China in the east within the southernmost CAOB. The orogen is located between the Tarim Craton to the south and the Junggar Basin to the north (Fig. 1). It was formed by long-lived Paleozoic subduction of the Paleo-Asian Ocean and accretions of several microcontinents (e.g., Yili Block, Chinese Central Tianshan Block, Ishim–Middle Tianshan in Kyrgyzstan, Aktau–Junggar in Kazakhstan, Gao et al., 2007, 2011; Kröner et al., 2012, 2013). In China, this orogenic belt is divided into four tectonic units, namely the Chinese North Tianshan (NT), the Yili Block (YB), the Chinese Central Tianshan Block (CTB) and the Chinese South Tianshan (ST) (Fig. 1) (Gao et al., 1998; Charvet et al., 2007; Gao et al., 2009; Charvet et al., 2011).

The NT and ST are Paleozoic accretionary terranes (Gao et al., 2009; Xiao et al., 2013; Alexeiev et al., 2015). The NT consists of Devonian–Carboniferous volcanic rocks, volcaniclastic rocks and turbidites (Wang et al., 2006). Carboniferous ophiolitic remnants (325–344 Ma) are exposed within the turbidites sequences (Xu et al., 2005; Wang et al., 2006). Permian molasse unconformably overlies the accretionary complex in this terrane (Zhu et al., 2013). The NT formed as a result of subduction of the North Tianshan Ocean. This ocean is considered to have closed in the late Carboniferous, based on the 316 Ma Sikeshu pluton intruding the ophiolite and the occurrence of post-collisional stitching intrusions (310–280 Ma) (Wang et al., 2006; Han et al., 2010). Likewise, the ST is mainly composed of Paleozoic clastic and volcano-sedimentary rocks (XBGMR, 1993; Chen et al., 1999a; Biske and Seltmann, 2010; Alexeiev et al., 2015). High pressure–low temperature (HP–LT) metamorphic assemblages (454–302 Ma) with relicts of blueschist, eclogite, ophiolite and meta-sedimentary rocks occur as tectonic lenses within the Paleozoic sedimentary strata (Gao et al., 1998; Zhang et al., 2003; Klemd et al., 2005; Gao et al., 2011; Klemd et al., 2011). The formation of the ST is considered to be the result of closure of the South Tianshan Ocean and Paleozoic collision between the Chinese Central Tianshan Block and the Tarim Craton (Gao et al., 2011; Xiao et al., 2013; Klemd et al., 2015).

The Yili Block and Chinese Central Tianshan Block are regarded as two major continental fragments or microcontinents involved in the formation of the Chinese Tianshan Orogen (Hu et al., 2000; Liu et al., 2004; Xiao et al., 2004; Xiao et al., 2008; Ma et al., 2012a,b, 2013; Wang et al., 2014a,c; Huang et al., 2015b). The Precambrian basement of the YB consists of granitic gneiss, fine-grained amphibolite and migmatite with meta-sedimentary covers including quartzite, slate, schist, leptynite and marble (926–650 Ma) (XBGMR, 1993; Chen et al., 1999b; Gao et al., 2009; Hu et al., 2010; Xiao et al., 2010; Huang et al., 2013; Liu et al., 2014; Wang et al., 2014a,b). Late Neoproterozoic (Sinian) tillite and Cambrian phosphorous limestone occur widely in this block. Early Paleozoic sedimentary rocks are rarely exposed on the surface, but late Paleozoic volcanic sedimentary rocks and clastic rocks occur throughout the YB (XBGMR, 1993; Huang et al., 2013; Xiao et al., 2013). Devonian rocks include conglomerates, sandstones, siltstones, mudstones, shales and limestones. The Carboniferous strata consist of sandstone, siltstone, limestone and volcanic rocks associated with andesite, rhyolite and dacite (XBGMR, 1993; Wang et al., 2007, 2008; Huang et al., 2013). Similarly, the CTB is characterized by a Precambrian basement overlain by Paleozoic clastic sediments and volcano–sedimentary rocks (Gao et al., 1998; Hu et al., 2000; Liu et al., 2004; Shu et al., 2004; Xiao et al., 2004; Gao et al., 2009; Lei et al., 2011; He et al., 2012; Shu et al., 2013; He et al., 2014c). In the western Chinese Central Tianshan Block (WCTB) (the CTB is divided into western and eastern parts along the Urumqi–Korla road), the Precambrian basement (969–707 Ma) is composed of migmatite, granitic gneiss with meta-sedimentary covers (XBGMR, 1993; Gao et al., 1998; Li et al., 2007; Chen et al., 2009; Long et al., 2011a; Ma et al., 2013). In the eastern Chinese Central Tianshan Block (ECTB), the basement rocks (1458–696 Ma) also consist of migmatite, gneiss with a clastic metasedimentary cover (Liu et al., 2004; Hu et al., 2010; Lei et al., 2013; Huang et al., 2014; He et al., 2014c; Wang et al., 2014c; Huang et al., 2015a,b). The entire CTB experienced five Precambrian magmatic events at ca. 1458–1400 Ma, 969–926 Ma, 945–880 Ma, 806 Ma and 740–707 Ma, and this block experienced a marked Mesoproterozoic crustal growth event (1.6–1.3 Ga) (Huang et al., 2015b).

Meta-sedimentary samples in this study were collected from the Wenquan Group of the Wenquan Metamorphic Complex (WMC) (Fig. 2) exposed in the northern Yili Block (Fig. 1). This complex extends for ca. 150 km from the Wenquan area to southeastern Kazakhstan (Wang et al., 2014a) and mainly consists of granitic gneiss, amphibolite, migmatite, paragneiss, leptynite, quartzite, schist, marble and slate (XBGMR, 1993; Hu et al., 2000, 2008; Wang et al., 2008; Hu et al., 2010; Wang et al., 2012; Huang et al., 2013; Liu et al., 2014; Wang et al., 2014a). Previously, these WMC basement rocks were considered to be Paleoproterozoic in age (XBGMR, 1993). However, available geochronological studies indicate that they formed at ca. 926–650 Ma instead of Paleoproterozoic (Hu et al., 2010; Li et al., 2013; Liu et al., 2014; Wang et al., 2014a). Noticeably, early Paleozoic strata are absent in the WMC, whereas late Paleozoic clastic rocks including sandstone, limestone and conglomerate are mostly exposed in its southern part. Although Neoproterozoic granitic rocks are limited to the central region of the WMC, early Paleozoic intrusive rocks widely occur westward at the northern margin of the WMC and late Paleozoic granitic–volcanic rocks are distributed in its southern part (Fig. 2). The above Neoproterozoic and early Paleozoic granitic rocks intruded into the Precambrian meta-sedimentary rocks (Fig. 2; Hu et al., 2008; Wang et al., 2012; Huang et al., 2013; Li et al., 2013; Wang et al., 2014a).

3. Sample description

Our samples were collected from the lower Wenquan Group (LWG) and the upper Wenquan Group (UWG) exposed within the Wenquan Metamorphic Complex, northern Yili Block (Fig. 2). Samples from the

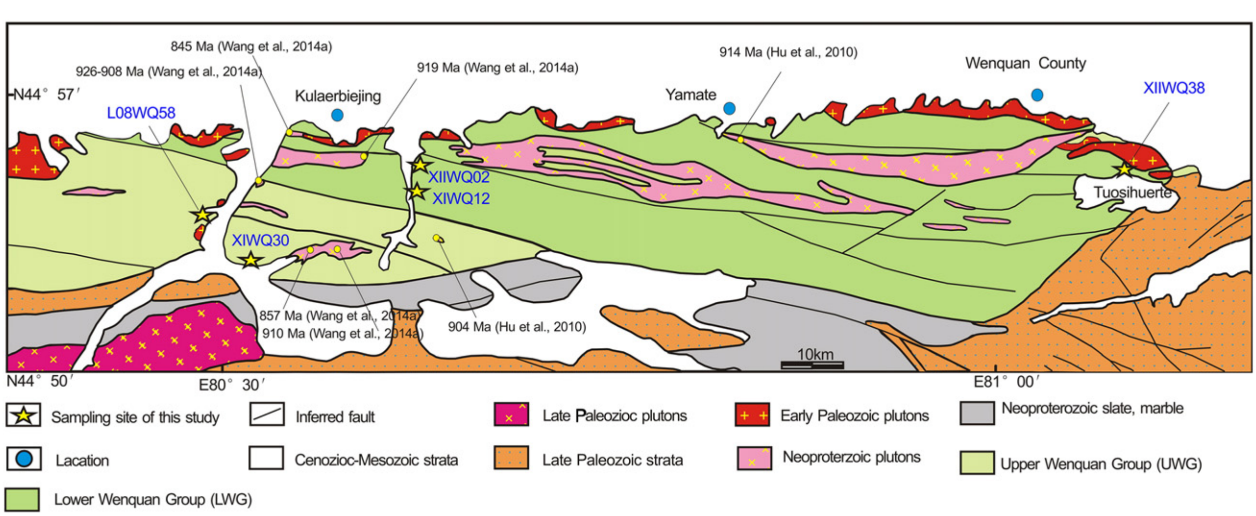

Fig. 2. Geological map of the Wenquan Metamorphic Complex with sampling locations marked. Modified after XBGMR (1993).

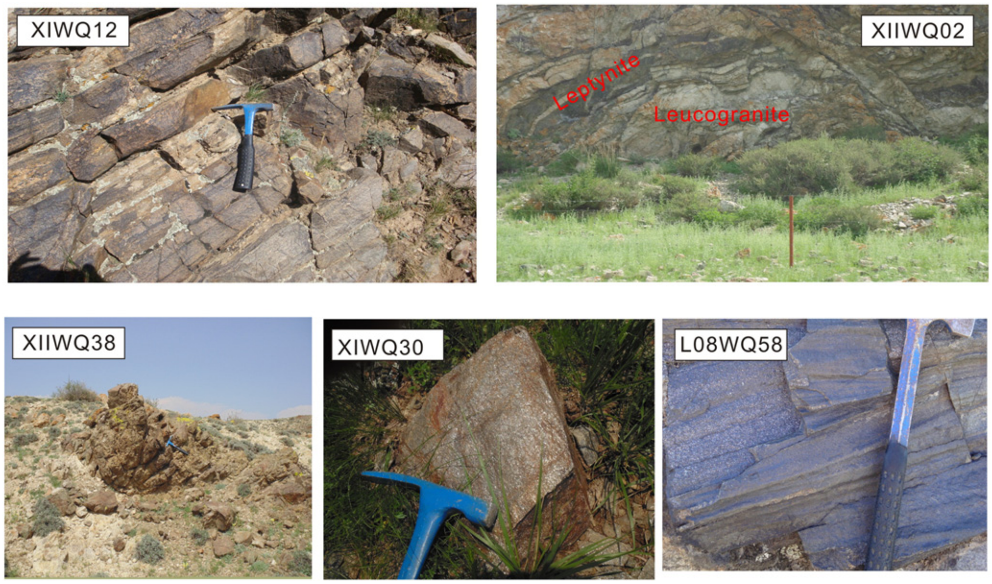

Fig. 3. Field photos of Neoproterozoic meta-sedimentary rocks in the Wenquan Metamorphic Complex, Yili Block. XIWQ12 is quartzite, XIIWQ02 and XIIWQ38 are leptynites. They are collected from the lower Wenquan Group (LWG). L08WQ58 and XIWQ30 are slate and quartzite, respectively. They both are collected from the upper Wenquan Group (UWG).

LWG consisted of medium-grained quartzite and leptynite, whereas medium-grained slate and quartzite were collected from the UWG. They are both intruded by Neoproterozoic and Paleozoic granitoids.

Quartzite from the LWG (sample: XIWQ12) is gray in color and displays bedding structure (Fig. 3). The quartzite mostly consists of quartz (~85%), with minor plagioclase and biotite or muscovite (~15%). The leptynite samples from the LWG (XIIWQ02 and XIIWQ38) are gray or brownish gray, mainly consisting of quartz (~65%) and plagioclase (~20%) and biotite (~15%). The slate sample from the UWG (L08WQ58) is mainly composed of quartz (~65%) and plagioclase (~25%) with minor biotite (~10%) (Fig. 3). The quartzite sample from the UWG (XIWQ30) exhibits slightly different petrological characteristics from those of the LWG (XIWQ12). In outcrop, sample XIIWQ02 is intruded by Neoproterozoic leucogranites, whereas sample XIIWQ38 occurs as lenses in Paleozoic granitic rocks (Fig. 3).

4. Analytical methods

Zircons were separated using heavy liquids and magnetic techniques, and were then handpicked under a binocular microscope. Zircon grains were mounted on adhesive tape and then enclosed in epoxy resin. The mounts were then polished to about half their thickness, and zircons were photographed under a microscope. In order to observe the internal structure of the polished zircons, cathodoluminescence (CL) imaging was carried out using a JXA-8100 Electron Probe Microanalyzer with a Mono CL3 Cathodoluminescence System for high resolution imaging and spectroscopy at the State Key Laboratory of Isotope Geochemistry, Guangzhou Institute of Geochemistry, Chinese Academy of Sciences (SKLIG GIGCAS).

4.1. Zircon U–Pb dating

U–Pb dating of samples was conducted using the LA-ICP-MS method in the same laboratory. Laser ablation was accomplished using a pulsed Resonetic 193 nm ArF excimer laser, operated at a constant energy of 80 mJ, with a repetition rate of 8 Hz and a spot diameter of 31 μm. The 91500 standard zircon, the Plesovice zircon and the NIST SRM 610 glass were used as standards. Specifically, 91500 was used as an external standard for correction of the isotopic ratios to calculate U–Pb ages; Plesovice was a monitoring standard, and the NIST SRM 610 glass was an external standard for elemental concentration analysis. The detailed analytical technique was described by Li et al. (2011). For samples, off-line inspection and integration of background and analysis signals as well as time-drift correction and quantitative calibration for trace element analyses and U–Pb dating were performed using Glitter 4.0 (Macquarie University). The age calculations and concordant plots were processed using ISOPLOT (version 3.0, Ludwig, 2003), and the analytical results are presented in Appendix A. Table 1.

4.2. Lu–Hf isotopic analysis

Hf-in-zircon isotopic analysis was performed using a Neptune Plus MC-CP-MS, coupled to the Resonetics RESOlution M-50-LR Excimer Laser Ablation System installed in the SKLIG GIGCAS. Hf isotopic data were acquired by ablating material from spots 45 μm in beam diameter, and a 8 Hz at 80 MJ repetition rate was used. The ablated material was transported by a helium carrier gas with mirror nitrogen. Data acquisition for each analysis consists of 30 s gas background collection and 30 s signal collection. A signal collection model for one block includes 200 cycles, and one cycle has an integration time of 0.131 s. The measured isotopic ratios of 176Hf/177Hf were normalized to 179Hf/177Hf = 0.7325, using exponential correction for mass bias. In order to obtain accurate 176Hf/177Hf ratios, the isobaric interferences of 176Lu and 176Yb on 176Hf must be corrected. The ratios of 176Lu/175Lu = 0.02655 and 176Yb/171Yb = 0.90184 obtained during Hf analysis on the same spot were used in the isobaric interference correction ((Machado and Simonetti, 2001; Wu et al., 2006). External corrections were applied to all unknowns, and the standard zircon Penglai were used as external standard and were analyzed twice before and after every 5 analyses of unknowns. The measured 176Lu/177Hf ratios and the 176Lu decay constant of 1.867×10^{-11} a^{-1} reported by Söderlund et al. (2004) were used to calculate initial 176Hf/177Hf ratios. Chondritic values of 176Hf/177Hf = 0.282772 and 176Lu/177Hf = 0.0332 reported by Blichert–Toft and Albarede (1997) were used for the calculation of ε_{Hf} (t) values. The depleted mantle line is defined by present–day 176Hf/177Hf = 0.28325 and 176Lu/ 177Hf = 0.0384 (Griffin et al., 2004). Because zircons formed in granitic magma are derived from felsic protoliths, two–stage (crustal) model ages (T^{C}_{DM}) are more meaningful than depleted mantle model ages. A mean 176Lu/177Hf ratio of 0.015 for the average continental crust (Griffin

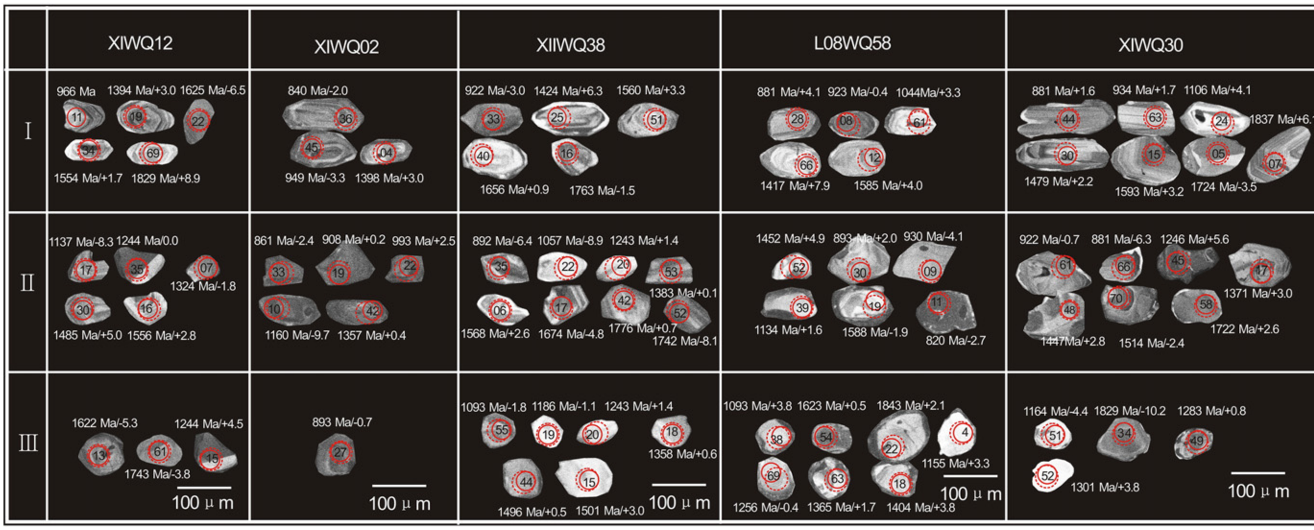

Fig. 4. Cathodo-luminescence images of detrital zircons of Neoproterozoic meta-sedimentary rocks. For further explanations see in the text.

et al., 2002) was used to calculate T^{C}_{DM}. The Lu–Hf isotopic data are listed in Appendix A. Table 2.

5. Results

5.1. Zircon features

All detrital zircons from the Wenquan Group have similar characteristics. They are generally colorless, transparent with length/width ratios of 2:1 (Fig. 4). Most also show relatively high Th/U ratios ($0.10 < Th/U < 1.0$) (Fig. 5), remarkably positive Ce anomalies as well as negative Eu anomalies and HREE enrichment relative to LREE (Appendix A. Table 3), which are a typical of magmatic origin (Hoskin and Schaltegger, 2003; Wu and Zheng, 2004). Three types of zircons from five meta-sedimentary samples can be recognized through CL imaging (Fig. 4). Type I zircon grains (represented by ~40% of the total analyzed grains) are long or short prismatic, euhedral, have very little rounding at their pyramidal terminations, and show well-developed oscillatory zoning. These features, along with relative high Th/U ratios ($0.1 < Th/U$), indicate that the zircon grains have an igneous origin, and suggest a local or near-source region. Type II zircons (representing ~32% of the total analyzed grains) are characterized by near euhedral or subhedral shape with oscillatory zoning in some grains. Few grains are low luminescent, but their high Th/U ratios suggest an igneous origin. The near-euhedral grains suggest that they experienced rather short transport, and their source areas are most probably not far from the depositional sites. Type III zircons (accounting for ~28% of the total analyzed grains) are well rounded without well-preserved oscillatory zoning. Some grains are highly luminescent and have nebulous zoning, whereas others show low luminescence rims and complicated internal textures. Among the studied zircons, the majority of grains with ages < 1.0 Ga and 1.6–1.3 Ga belong to both type I and type II. However, most zircons with ages between 1.2 and 1.1 Ga are type III. The 1.85–1.7 Ga grains are more type I and type II than those of type III.

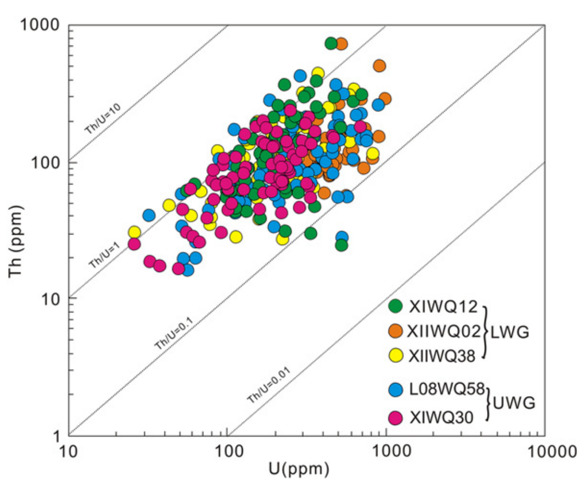

Fig. 5. Th–U plots of concordant zircons from all studied samples.

5.2. U–Pb ages and Hf isotopic compositions

In this study, 350 detrital zircons from five samples of the Wenquan Group were dated. Data with > 10% discordance and large uncertainties (> 100 Ma at 1σ uncertainties of 207Pb/206Pb ages) are excluded in the following discussion (Appendix A. Table 1). Because 206Pb/238U ages are generally more precise for young zircons and 207Pb/206Pb ages for older ones, we rely on the measured 207Pb/206Pb ages when 206Pb/238U ages are older than 1000 Ma. Concordant analyses were selected for in-situ Hf isotope measurement (Fig. 4 and Appendix A. Table 2).

5.2.1. Quartzite of the lower Wenquan Group (LWG: XIWQ12)

Seventy zircons were dated for sample XIWQ12, and 40 grains are concordant within error. The dominant zircon population yielded ages between 1320 and 1600 Ma (Fig. 6a), whereas others exhibited a younger age peak at 950 Ma (Fig. 7a). Thirty-five zircon crystals were also analyzed for their Hf isotopic compositions. The $\varepsilon_{Hf}(t)$ values vary from to -8.3 to $+8.9$ with crustal model ages (T^{C}_{DM}) from 2.78 to 1.77 Ga (Fig. 8a).

5.2.2. Leptynite of the lower Wenquan Group (LWG: XIIWQ02 and XIIWQ38)

Sixty analyses of sample XIIWQ02 yielded 51 concordant grains ranging from 1660 to 817 Ma (Fig. 6b). The main population gave ages between 996 Ma and 817 Ma, forming a major peak at 900 Ma (Fig. 7b). Fifty of the above zircons were analyzed for Hf isotopic compositions. They yielded relatively low initial 176Hf/177Hf ratios with a large variation in $\varepsilon_{Hf}(t)$ values (-15.5 to $+3.0$) (Fig. 8a) and old crustal model ages ($T^{C}_{DM} = 2.73$–1.70 Ga).

For sample XIIWQ38, seventy zircons were dated, and 68 grains are concordant within error. The results show similar age spectra to that of sample XIWQ12 (Fig. 6a and c). The dominant zircon population gives

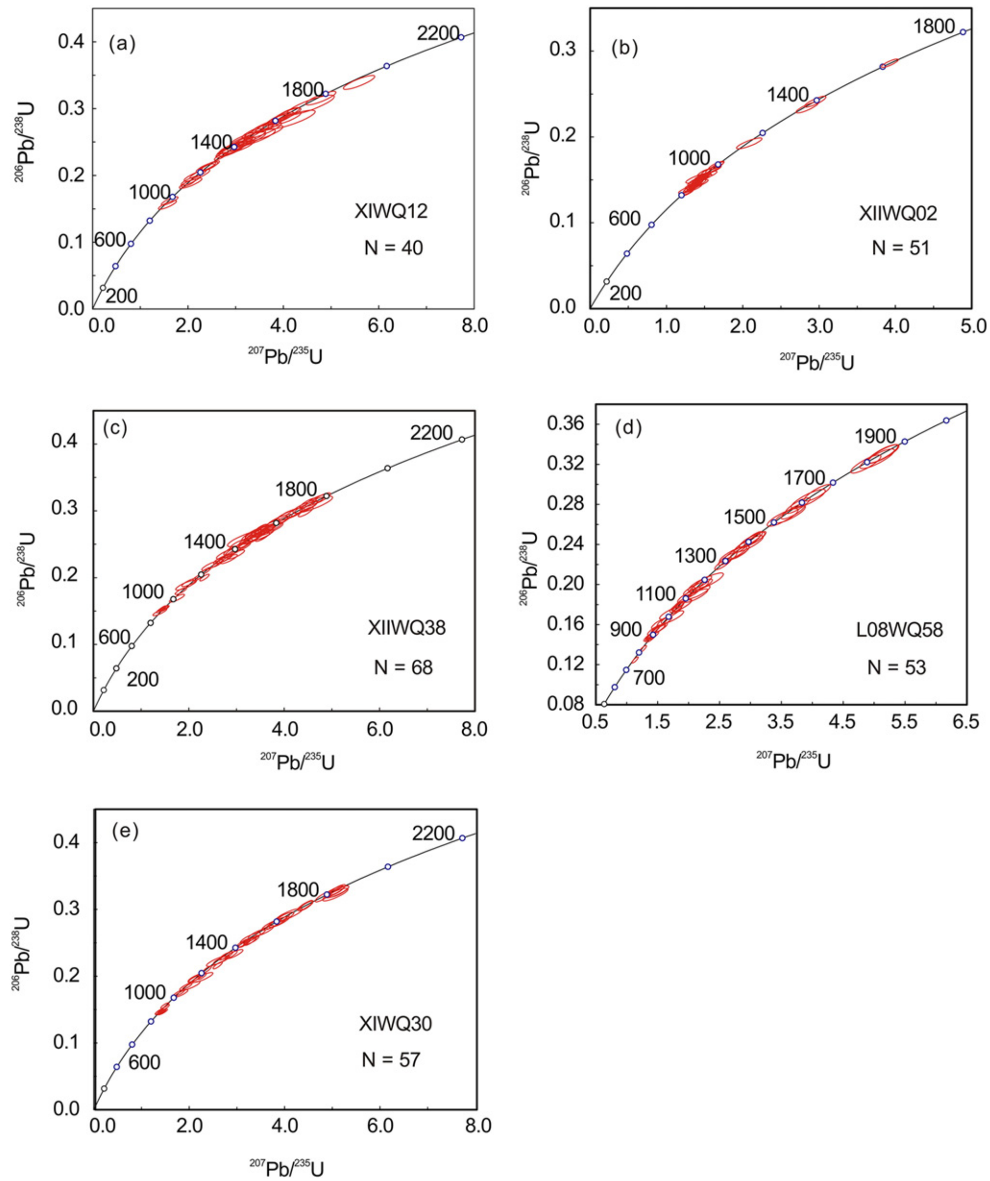

Fig. 6. Zircon U–Pb concordia diagrams with concordant analyses for the five Neoproterozoic meta-sedimentary rocks in the Yili Block.

ages between 1370 Ma and 1600 Ma, and the youngest age peak is at 920 Ma (Fig. 6c). Forty–seven zircon crystals were also analyzed for their Hf isotopic composition. Comparing with sample XIWQ12, these zircons display more variable initial 176Hf/177Hf ratios and thus show various ε_{Hf} (t) values (−11.8 to +7.0) and slightly older crustal model ages (T_{DM}^{C} = 3.17–1.71 Ga) (Fig. 8a).

5.2.3. Slate of the upper Wenquan Group (UWG: L08WQ58)

Eighty zircons of sample L08WQ58 were analyzed for U–Pb isotopic composition. Fifty–three grains are concordant varying from 1849 to 758 Ma (Fig. 6d), with two major age peaks at 890 and 930 Ma (Fig. 7d). There are several minor age peaks between 1180 and 1840 Ma (Fig. 7d). Fifty zircons were analyzed for Hf isotopic composition. These analyses have a wide range of ε_{Hf} (t) values ranging from −9.8 to +7.9 (Fig. 8b) with relatively young T_{DM}^{C} ages (2.51–1.54 Ga).

5.2.4. Quartzite of the upper Wenquan Group (UWG: XIWQ30)

Seventy zircons were dated, and 57 grains are concordant within error. The main zircon population gave ages between 1864 and 881 Ma (Fig. 6e), with a predominant age peak at 880 Ma and some minor age peaks between 1130 and 1850 Ma (Fig. 7e). In addition, three zircons yielded Neoarchean ages at 2604, 2647 and 2744 Ma (Fig. 7e). Analogous to sample L08WQ58, these zircons are characterized by highly variable ε_{Hf} (t) values (−13.0 to +7.3) (Fig. 8b) with relatively old T_{DM}^{C} ages (3.15–1.67 Ga).

6. Discussion

6.1. Depositional age of the Wenquan Group

The Wenquan Group within the Wenquan Metamorphic Complex was considered to be the oldest sequence in this complex and constituted the basement of the Yili Block. Previously, according to the microfossils, lithologic and structural relationships, the meta-sedimentary sequences of the Wenquan Group were originally considered to be Paleoproterozoic in age (XBGMR, 1993). However, recent geochronological studies revealed that the metamorphic rocks of the basement formed in the early Neoproterozoic rather than Paleoproterozoic (Hu et al., 2010; Liu et al., 2014; Wang et al., 2014a). These new data imply that the meta-sedimentary sequences were deposited later than previously estimated.

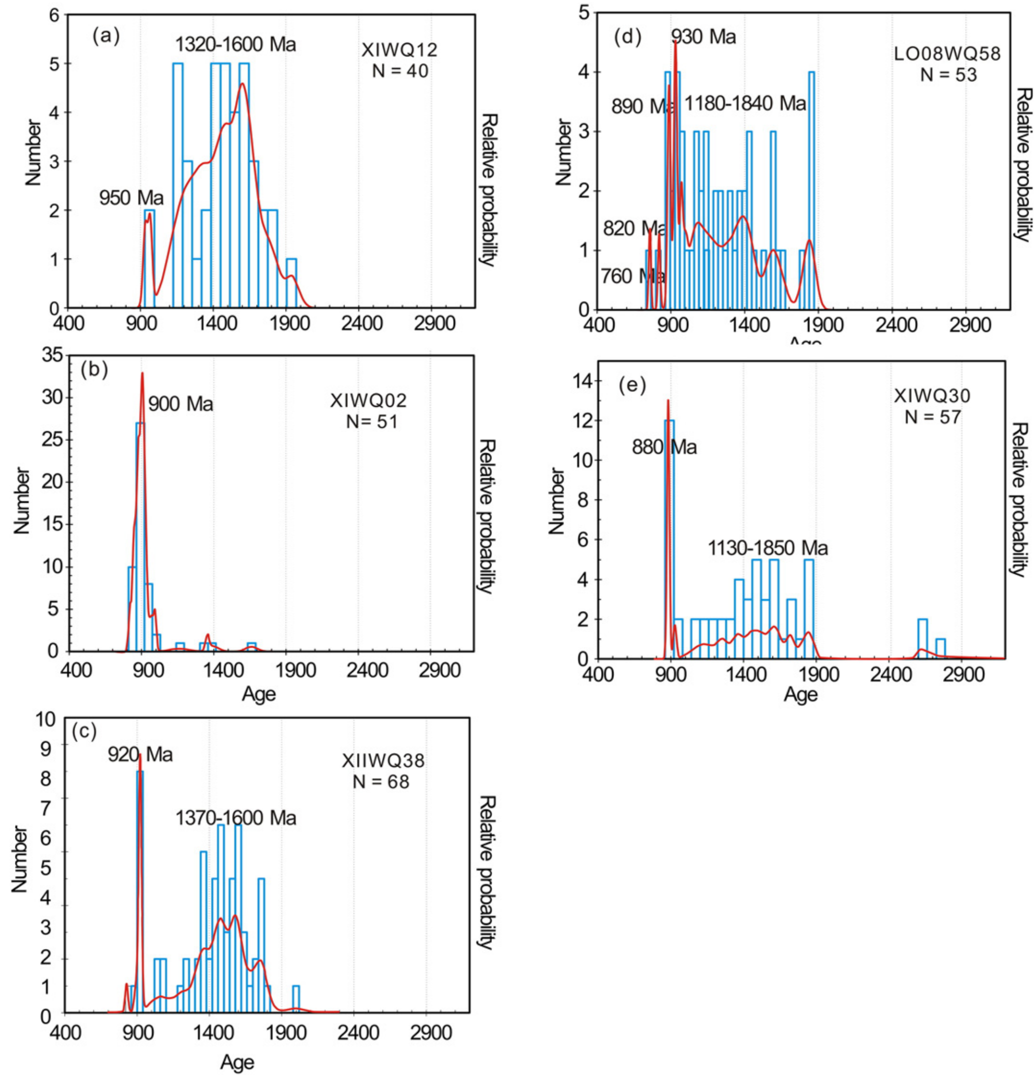

Fig. 7. Relative U–Pb age probability for concordant detrital zircons from five samples in the Yili Block.

Because the time of deposition should not be older than the youngest detrital zircon, the age peak of the youngest group can be used to constrain the maximum age of deposition (Nelson, 2001; Fedo et al., 2003; Gehrels, 2014). The youngest zircon 206Pb/238U age populations from quartzite and leptynite samples of the LWG peak at 900, 920 and 950 Ma, respectively (Fig. 7a–c), suggesting that the maximum depositional age of the LWG was not prior to ca. 900 Ma. Some leucogranites intruded into these meta-sedimentary rocks, and dating of these granitoids yielded a weighted mean age of 845 ± 8 Ma (Wang et al., 2014a, Fig. 2), which suggests that the metasediments must have been deposited before this age. Therefore, the LWG was probably deposited during the early Neoproterozoic (900–845 Ma).

Two meta-sedimentary rocks of the so-called UWG have similar age distributions with marked peaks at 880 Ma and 890 Ma, respectively (Fig. 7d and e). The two youngest detrital zircons were dated at ca. 820 Ma and 760 Ma (Fig. 7d). However, the internal textures of these two zircon crystals are low luminescent and have nebulous zoning (Fig. 4, spot 11 of L08WQ58) with relatively higher U contents than other detrital zircons (539–617 ppm) (Appendix A. Table 1). This means that these two grains have experienced Pb loss. Thus, these two young ages could not represent the maximum depositional age of the UWG. Alternatively, peaks at 880 Ma and 890 Ma are the best choices to constrain the depositional age. Therefore, deposition of the UWG probably occurred at ca. 880 Ma. A slightly younger orthogneiss (857 ± 6 Ma) near the base of this sequence intruded into the UWG (Wang et al., 2014a, Fig. 2), which suggests that the UWG was deposited before this age. Therefore, the UWG was deposited during the early Neoproterozoic (880–857 Ma), later than the LWG of the Wenquan Metamorphic Complex in the Yili Block.

6.2. Sedimentary provenance

Detrital zircons from three samples (XIWQ12, XIIWQ02 and XIIWQ38) of the lower Wenquan Group (LWG) display similar youngest Neoproterozoic age peaks (950 Ma, 900 Ma and 920 Ma, respectively) (Fig. 7a–c). Additionally, sample XIIWQ38 has similar age peaks to the quartzite (XIWQ12) between 1320 Ma and 1600 Ma (Fig. 7a and c). However, a small differences shows up on the age peaks after the Neoproterozoic for XIIWQ02, compared to the other two samples. This sample has few Mesoproterozoic age peaks. Although samples XIIWQ02 and XIIWQ38 have similar mineral compositions, the zircons of sample XIIWQ02 have less pre-Neoproterozoic information than those of sample XIIWQ38. This can probably be attributed to the depositional environments for synchronous sedimentation or a progressive change of sedimentary facies with reducing input of older deep-seated material with time. Nevertheless, despite these minor differences between the samples, the source character of the LWG is

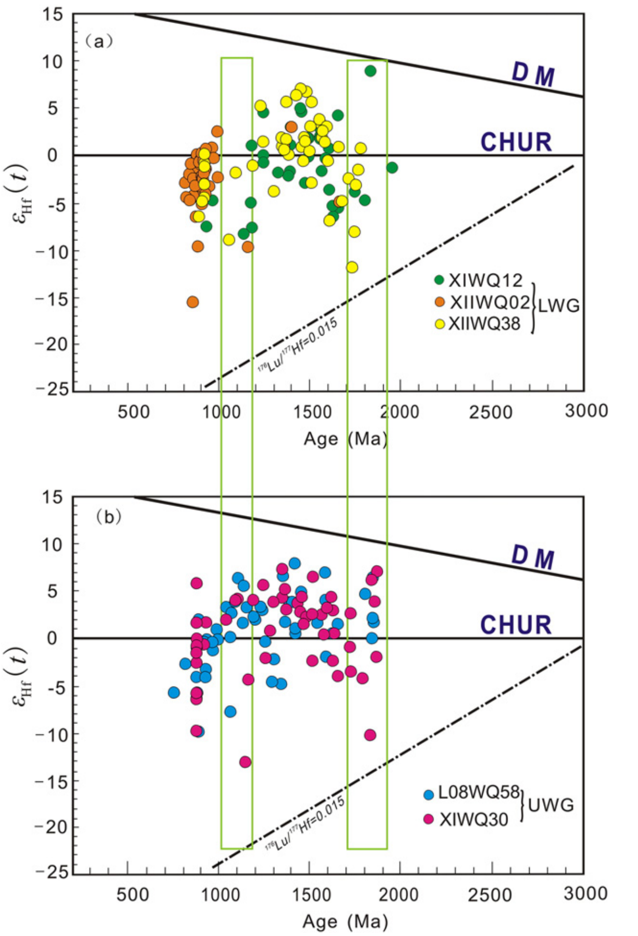

Fig. 8. Diagram of ε_{Hf} (t) value vs. age for concordant detrital zircons from the Neoproterozoic meta-sedimentary rocks.

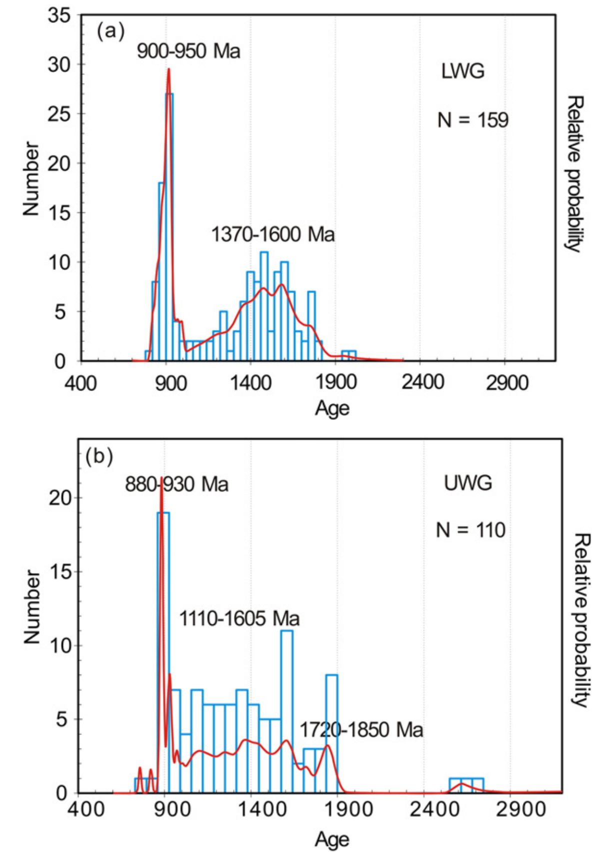

Fig. 9. Distribution of concordant detrital zircon U–Pb analyses for the five samples. (a) Age distribution pattern for the samples from the lower Wenquan Group (LWG). (b) Age distribution pattern for the samples from the upper Wenquan Group (UWG).

reflected by these three samples, including two age periods at ca. 900–950 Ma and 1370–1600 Ma, respectively (Fig. 9a).

Detrital zircons from the meta-sedimentary rocks of the UWG define similar multi-peake zircon age distribution patterns at 880–930 Ma and 1130–1850 Ma with a weak age peak at 2620 Ma (Fig. 7d and e). It is obvious that detrital zircons from the UWG and LWG exhibit analogous age distribution patterns at 880–950 Ma and 1370–1600 Ma (Fig. 9a and b). However, the UWG has distinct age distributions at ca. 1100 Ma and 1720–1850 Ma (Fig. 9a and b). These data may suggest that the UWG metasediments inherited some material from the LWG (e.g., 880–950 and 1370–1600 Ma), but had an input of new source material with ages of ~1100 Ma and 1720–1850 Ma, probably due to a different depositional environment. This is also evidenced by the different Hf isotopic characteristics of detrital zircons. The 1720–1850 Ma grains from the UWG have more positive ε_{Hf} (t) values than those from the LWG (Fig. 8a and b).

The early Neoproterozoic zircon population (especially that at ca. 0.95–0.88 Ga) from the LWG and UWG shares similar source material. Most detrital zircons of this population show concentric zoning and high Th/U ratios, which are consistent with an igneous origin. Their euhedral and prismatic morphologies infer that these zircons experienced short sedimentary transport and are probably related to a proximal magmatic source (Fig. 4). Noticeably, these zircons exhibit a large variation of Hf isotopic compositions with ε_{Hf} (t) values mostly between −15.5 and +2.5 (Fig. 8a and b). It seems that the zircons with positive ε_{Hf} (t) values may originate from isotopically primitive rocks. However, their euhedral and prismatic shapes with significant oscillatory zoning indicate derivation from granitoid rocks possibly with additions of mantle-derived material when or before the granitoid rocks formed. Recent studies revealed that several early Neoproterozoic S-type granitoids are exposed in the Yili Block (Fig. 2; Chen et al., 1999b; Hu et al., 2010; Li et al., 2013; Wang et al., 2014a). Most of these peraluminous rocks were dated at 926–845 Ma with ε_{Nd} (t) values of −1.9 to −9.1 (Wang et al., 2014a). Therefore, locally exposed S-type granites have probably provided a large proportion of the clastic material for the early Neoproterozoic zircons dated in this study.

Mesoproterozoic detrital zircons from the Wenquan Group are more complex than the Neoproterozoic grains (especially ca.1.60–1.37 Ga for both LWG and UWG, and ~1.1 Ga for the UWG). For the additional ~1.1 Ga zircons of the UWG, Hf isotopic compositions indicate that juvenile or inherited material was largely involved in the source of the UWG (Fig. 8a and b). As to the ca. 1.60–1.37 Ga zircons, they were consistently identified in both the LWG and UWG with similar ε_{Hf} (t) values between −6.9 and +7.9 (Fig. 8a and b), suggesting a similar provenance. Noticeably, positive ε_{Hf}(t) values occupy 75% of all analyses of this population, indicating that more juvenile than crustal material contributed to the source of the LWG and the UWG at 1.60–1.37 Ga. Considering the morphologies of most of these detrital zircons (Fig. 4) and their isotopic data, the contribution of local material from the Yili Block (YB) and material from the Chinese Central Tianshan Block (CTB) may have contributed significantly to the provenance of the Mesoproterozoic detrital zircons. This is supported by sporadically occurring 1.33 and ~1.0 Ga magmatic rocks in the Yili Block (our unpublished data) and 1.46–1.40 Ga gneissic granitoids in the CTB (Huang et al., 2015b).

It would appear that the Siberian Craton, the Tuva Mongolia terrane, the Tarim Craton, the Kazakhstan–Kyrgyzstan Tianshan, and the North China Craton could also be potential sources for the 1.60–1.37 Ga and ~1.1 Ga detrital zircons. However, the absence of magmatic rocks of these ages in the Siberian Craton, Tuva–Mogolia and the Tarim

Craton (Badarch et al., 2002; Poller et al., 2005; Xu et al., 2013; Zhang et al., 2013a) rules out these continents as potential sources. A few 1.6–1.4 Ga granitoids are exposed in the Kyrgyzstan North Tianshan (Kröner et al., 2013), but their zircons show negative isotopic signatures different from those of the LWG and the UWG (Fig. 8). Thus, the Kyrgyzstan Tianshan could be excluded. Although 1.4–1.3 Ga diabase or bimodal rocks are exposed in the North China and South China cratons (Li et al., 2002b; Zhang et al., 2012c; Li et al., 2014), zircons from diabase have internal features or ε_{Hf} (t) values distinct from the coeval detrital zircons in this study. This suggests that the two cratons also cannot be the sources for the 1.6–1.4 Ga detrital zircons. For ~1.1 Ga detrital zircons, the South China Craton could potentially be provenance because of ~1.1 Ga basalts (Greentree et al., 2006; Qiu et al., 2011), but their different negative ε_{Nd} (t) values exclude this possibility.

Late Paleoproterozoic detrital zircons (1.85–1.72 Ga) dominate in the UWG. Two possible interpretations are suggested for their provenance: local concealed magmatic rocks or long-distance transport from nearby old blocks. In recent years, not only late Paleoproterozoic (~1.8 Ga) but also voluminous latest Archean (~2.5 Ga) igneous rocks have been discovered in the surrounding old blocks, such as the Siberian Craton, the North China Craton and the Tarim Craton (Zhai, 2004; Xiong et al., 2009; Zhao et al., 2010). If the studied Paleoproterozoic detrital grains were derived from any of these cratons, numerous >1.8 Ga detrital grains (e.g., ~2.5 Ga grains) would be expected in the Wenquan metasediments. However, because such old detrital zircons are nearly absent in the Yili Block (Fig. 11), the second interpretation can be excluded. Therefore, we suggests that the Paleoproterozoic detrital grains were most likely derived from an unknown local source which is in agreement with other recent studies (Liu et al., 2014; He et al., 2015).

6.3. Crustal evolution of the Yili Block

Juvenile and evolved isotopic characteristics of granitoid rocks are vital for recognizing crustal growth and ancient crustal reworking in the Precambrian (Taylor and McLennan, 2009; Condie, 2011; Dhuime et al., 2011). However, Precambrian granitoid rocks have sometimes not been discovered in some microcontinents, which may hinder an understanding of the crustal evolutionary history. Likewise, Precambrian granitoid rocks are rare in the Yili Block. Although recent studies demonstrated that Neoproterozoic granitoids are present in the basement (Hu et al., 2010; Li et al., 2013; Wang et al., 2014a), few data support the existence of Paleoproterozoic or Mesoproterozoic rocks.

As discussed above, our provenance study indicates that the most detrital zircons are near or locally derived. This conclusion provides a way to decipher the crustal evolution of the Yili Block when old

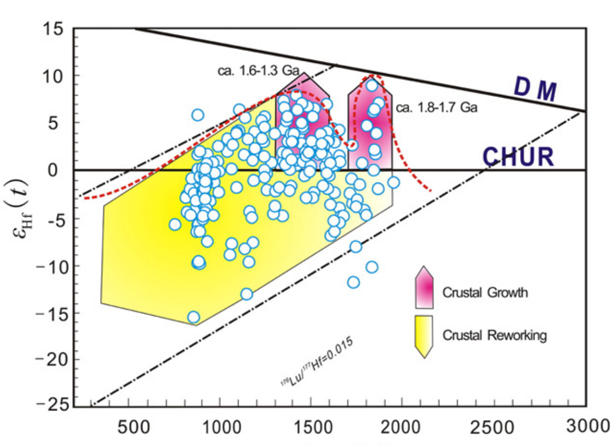

Fig. 10. Diagram of ε_{Hf} (t) value vs. age for concordant detrital zircons showing the crustal growth and reworking events in the Yili Block.

igneous rocks are very limited or have not to be well identified. Our Hf isotopic data indicate that the late Paleoproterozoic zircons (1.85–1.72 Ga) mostly have juvenile ε_{Hf} (t) values (Fig. 10). Among these grains, 60% with such positive values are euhedral or near euhedral to subhedral, which confirms that these grains are most likely local, and a late Paleoproterozoic basement is likely to exist at depth in the Yili Block. Their positive ε_{Hf} (t) values therefore represent late Paleoproterozoic juvenile crustal material in the Yili Block (Fig. 10). It is noticeable that there are still 40% detrital zircons with negative ε_{Hf} (t) values, which indicate synchronous crustal reworking. Hf crustal model ages of the local grains vary between ca. 2.95 Ma and 1.94 Ma (Appendix A. Table 2). This implies that some crustal material in the Yili Block formed as early as the Neoarchean.

Similarly, the majority of early Mesoproterozoic detrital grains (1.6–1.3 Ga) have positive ε_{Hf} (t) values (Figs. 4 and 10). These characteristics indicate that early Mesoproterozoic crustal growth occurred in the Yili Block as well. The late Paleoproterozoic and early Mesoproterozoic local zircon grains define a crustal evolution trend, and most Mesoproterozoic to Neoproterozoic grains plot within this trend (Figs. 4 and 10). This suggests that Mesoproterozoic to Neoproterozoic grains with moderate to negative ε_{Hf} (t) values were generated by crustal reworking. Although a few Mesoproterozoic (1.6–1.1 Ga) and Neoproterozoic (1.0–0.88 Ga) detrital zircons may be derived from the nearby CTB, most are originated from the local sources (Fig. 4 and part 5.1). It is reasonable to suggest that crustal reworking occurred in the Yili Block from the early Mesoproterozoic (1.6 Ga) to the Neoproterozoic (0.88 Ga) (Fig. 10). Therefore, we suggest that both synchronous crustal growth and reworking happened in the early Mesoproterozoic (1.6–1.3 Ga), and then changed into continuous crustal reworking until the early Neoproterozoic (Fig. 10).

6.4. Tectonic affinity of the Yili Block

The tectonic affinity of microcontinents within the CAOB has been the subject of much controversy. The Siberian Craton is considered to be the origin for some microcontinents within the CAOB (Berzin and Dobretsov, 1994; Sengör and Natal'in, 1996; Turkina et al., 2007). However, these rocks were also argued to have rifted from the Gondwana (Zonenshain et al., 1990; Dobretsov et al., 2003; Laurent-Charvet et al., 2003; Xiao et al., 2010). The Tarim Craton as a block rifted from Gondwana was thus widely considered to the origin of some microcontinents within the CAOB. (Li et al., 2008; Levashova et al., 2009; Lei et al., 2011; Levashova et al., 2011; Rojas-Agramonte et al., 2011; Shu et al., 2011; Ma et al., 2012a,b; Lei et al., 2013; Ma et al., 2013; Metcalfe, 2013; Liu et al., 2014; Rojas-Agramonte et al., 2014; Zhao et al., 2014; Wang et al., 2014c).

Recent studies suggest that the YB and the Chinese Central Tianshan Block (CTB) were likely derived from a same old continent (Qian et al., 2009; Liu et al., 2014; Huang et al., 2015b). However, some researchers considered that the YB has no relationship with the CTB, because the CTB was an independent continental block (Hu et al., 2000; Liu et al., 2004; Li et al., 2009). However, the detrital zircon grains of this study suggest that the YB and the CTB originated from the same old continent because the Yili Block and the CTB yielded similar age patterns with peaks at ca. 880, 920 and 1400–1600 Ma (Fig. 11a and b) (this study and He et al., 2014c). Additionally, detrital grains from the YB and the CTB have analogous ε_{Hf}(t) values (Fig. 12) (this study and He et al., 2014c), which further indicates that these two blocks have a joint single basement. Their similarity is also supported by the following considerations: (1) The Yili Block and CTB contain similar Precambrian rocks that mainly consist of granitic gneiss, migmatite, quartzite, marble, slate and various schists (XBGMR, 1993; Gao et al., 1998; Shu et al., 2004; Gao et al., 2009; Xiao et al., 2010; Huang et al., 2013; Shu et al., 2013). (2) Contemporaneous granitoid events are exposed in both blocks. For example, crustal magmatism at 939–845 Ma is

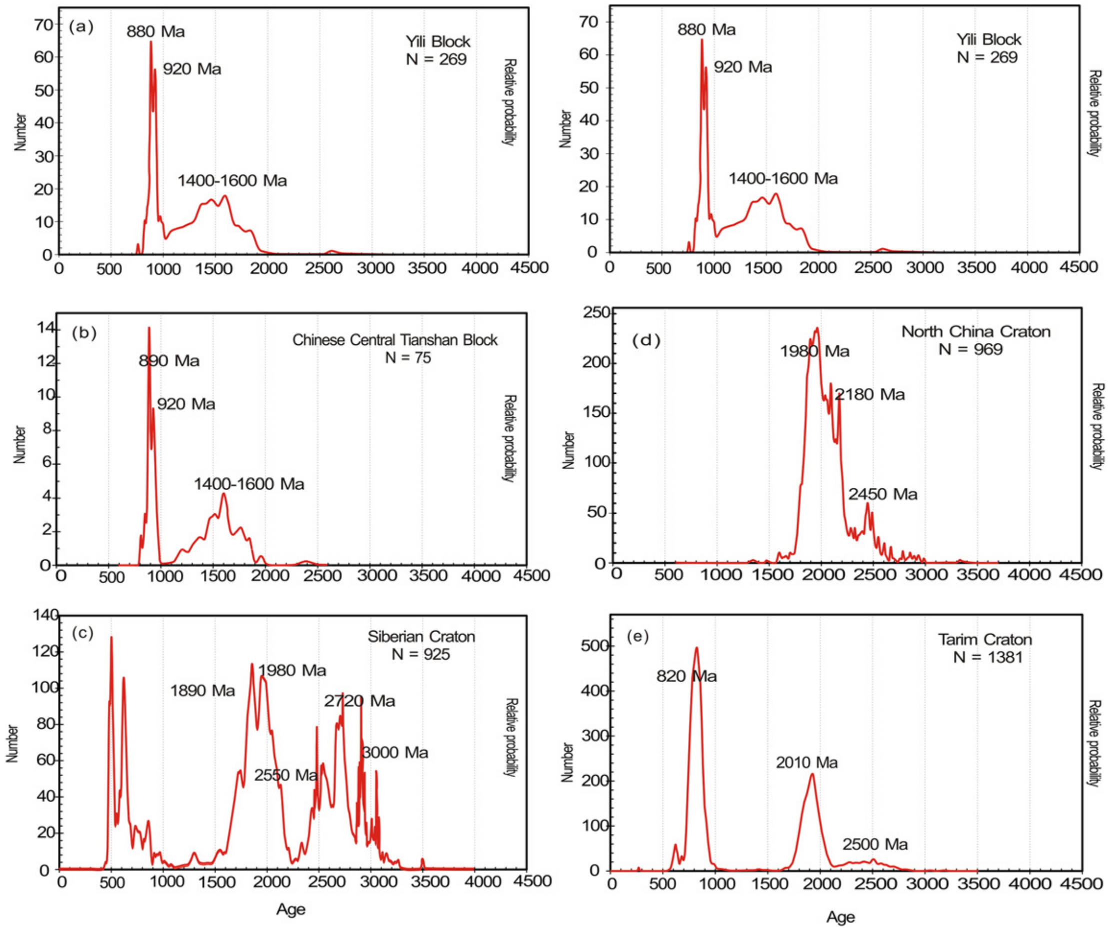

Fig. 11. Precambrian age distributions for the Yili Block, Chinese Central Tianshan Block, Siberian Craton, North China Craton and Tarim Craton (data from this study, Khudoley et al., 2001; Wan et al., 2006; Xia et al., 2006a,b; Luo et al., 2008; Zhu et al., 2011; Glorie et al., 2014; He et al., 2014a,b,c; Powerman et al., 2015).

recorded in the Yili Block (Hu et al., 2010; Li et al., 2013; Wang et al., 2014a). Magmatic rocks at 942–880 Ma resembling those in the YB also occur in the CTB and likely originated from sedimentary sources (Huang et al., 2014, 2015a,b). Neoproterozoic gneisses in the Yili Block

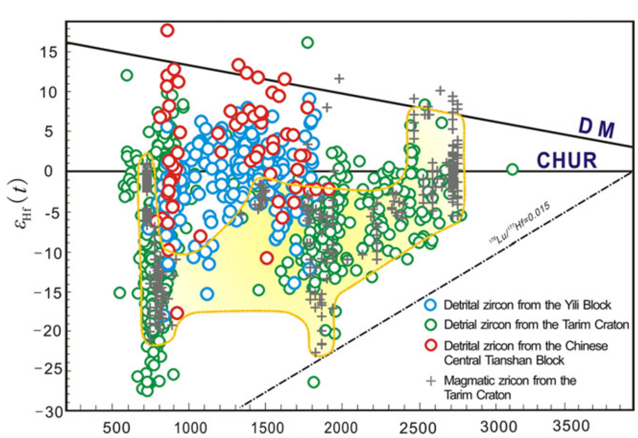

Fig. 12. Hf-in-zircon isotope evolution diagram for the Yili Block (this study), Chinese Central Tianshan Block (He et al., 2014c) and the Tarim Craton (He et al., 2014a,b). Yellow shaded field with cross mark indicates crustal evolution trend for the Tarim Craton, which is defined by the zircons from igneous rocks. (data from Long et al., 2010, 2011b,c; Lei et al., 2012; Zhang et al., 2012b; He et al., 2013; Ge et al., 2014; Wu et al., 2014).

have negative ε_{Nd} (t) values (−1.9 to −4.4) (Wang et al., 2014a), which are similar to the Hf isotopic signatures (−10.9 to 0) of magmatic rocks in the CTB (Huang et al., 2015b). This implies that they were derived from similar magma sources and formed in similar tectonic settings. (3) These blocks have experienced the same tectono-thermal events at 930–900 Ma. Migmatization occurred at 926–909 Ma in the Yili Block (Hu et al., 2010; Wang et al., 2014a), and most granitoid gneisses in this period have augen textures. Similarly, most Neoproterozoic granitoid rocks in the CTB show augen or banded textures, associated with a coeval anatectic event (ca. 900 Ma) (Huang et al., 2015b). Therefore, it is reasonable to conclude that the Yili Block and the Chinese Central Tianshan Block had a close tectonic affinity in the pre-Neoproterozoic. This conclusion is also supported by our study of Precambrian granitoid gneisses exposed in the Chinese Central Tianshan Block (Huang et al., 2015b).

Concerning the tectonic affinity between the Yili Block and the Siberian and North China cratons, the age spectra of detrital zircon grains from these two cratons are obviously different from those of the Yili Block. In the Siberian Craton, the age distribution is dominated by zircon crystals formed at 3.5–1.5 Ga with peaks at 1.89, 1.98, 2.55, 2.72 and 3.0 Ga (Fig. 11c) (Khudoley et al., 2001; Rojas-Agramonte et al., 2011; Glorie et al., 2014; Powerman et al., 2015). Similarly, in the North China Craton, the age population dominantly formed between 3.5 and 1.5 Ga with spikes at 1.98, 2.18 and 2.45 Ga (Fig. 11d) (Wan et al., 2006; Xia et al., 2006a, 2006b; Luo et al., 2008). Conversely, the Yili Block displays age populations varying from 2.0 to 0.8 Ga with age peaks at 880, 920 and 1.4–1.6 Ga (Fig. 11a). These imply that the

Siberian Craton and the North China Craton could not be the origin of the Yili Block. In the Siberian Craton, the oldest rocks yielded zircon ages of 3.6–3.2 Ga (Turkina et al., 2007; Gladkochub and Donskaya, 2009). The age peaks at 1.98 and 1.89 Ga are related to the assembly of the Siberian Craton (Rosen et al., 1994). After the Siberian basement stabilization at 1.9–1.8 Ga, the Siberian Craton was in an extensional environment with volcanic–plutonic rocks at ~1.73–1.68 Ga (Gladkochub et al., 2006). However, such geological facts mentioned above are not recorded in the detrital zircon grains of the Yili Block, and the basement of the YB shows no similarities with the Craton. Moreover, Siberian Craton had low paleo-latitudes at 770 Ma relative to placement adjacent to the CAOB (Levashova et al., 2011). Thus, the Siberian Craton could be excluded for the origin for the Yili Block. Likewise, in the North China Craton, the oldest crustal rocks were found with age of 3.8 Ga (Wan et al., 2005; Wu et al., 2008). After its cratonization at 1.85–1.80 Ga (Zhai, 2004; Zhao et al., 2010), this Craton experienced late Paleoproterozoic extension, and mafic dyke swarms with anorthosite–mangerite–alkali granitoid–rapakivi granite (1.78–1.68 Ga) are widespread in its northern and central parts (Peng et al., 2007, 2008; Zhao, 2009). However, although the detrital zircon grains in the Yili Block have recorded the ages from 1.8–1.6 Ga, no evidence shows that these ages are related to the cratonization of the North China Craton and a rifted environment. Moreover, mid–Mesoproterozoic bimodal magmatic rocks (1.4–1.2 Ga) have been reported from the North China Craton (Zhang et al., 2012c), but rocks in the Yili Block of this period are granitic rocks that are not consistent with a continental rift setting. Furthermore, both the Siberian Craton and the North China Craton are lacking of 1.2–0.8 Ga detrital zircon grains (Fig. 11a–d) and coeval granitic rocks in their basements. Thus, we suppose that the Yili Block was unlikely to rift from these two cratons in the Precambrian.

As to the tectonic affinity between the YB and Tarim Craton, these two blocks also have different age distribution patterns (this study and Zhu et al., 2011; He et al., 2014a,b). There are two major age peaks at 2.01 Ga and 2.5 Ga in the Tarim Craton, whereas these two peaks are absent in the Yili Block (Fig. 11a and e). Additionally, lacking of 1.6–1.4 Ga age peaks in the Tarim Craton indicates that these two blocks have experienced different tectono-thermal events (Fig. 11a and e). Furthermore, ε_{Hf} (t) values from detrital grains in the YB are distinctly different from those of the Tarim Craton (Fig. 12, He et al., 2014a,b). In Fig.12, ε_{Hf} (t) values of the igneous rocks and detrital zircon grains of the Tarim Craton match well with each other and define a specific crustal evolution trend (Fig. 12) (Long et al., 2010; Zhu et al., 2011; Long et al., 2011b,c; Lei et al., 2012; Zhang et al., 2012b; He et al., 2013; Ge et al., 2014; Wu et al., 2014; He et al., 2014a,b). This conclusively demonstrates that the detrital grains in the Tarim Craton were derived from a local source, and ε_{Hf} (t) values of these detrital zircons and the igneous rocks perfectly represent the Hf isotopic compositions of the Craton. Assuming that the YB was rifted off the Tarim Craton, the detrital grains could reflect similar isotopic characteristics as detrital grains and igneous rocks of the Tarim craton (Fig. 12). However, the 1.8–1.0 Ga detrital zircon crystals do not plot along this time-evolved trend, but show a distinctly different trend. This implies that the YB is unlikely to have been derived from the Tarim Craton. Moreover, two crustal growth events occurred in the Yili Block at ca. 1.8–1.7 and 1.6–1.3 Ga (Fig. 10). In contrast, the Tarim Craton was dominated by crustal reworking events in these periods (He et al., 2014a,b). It is therefore suggested that the Yili Block has no tectonic relationship with the Tarim Craton. This interpretation is also consistent with the fact that Neoarchean tonalite–trondhjemite–granodiorite suites and Paleoproterozoic metamorphism are absent in the YB. However, such rocks are exposed on the northern and southern margins of the Tarim Craton and experienced metamorphism at 2.0–1.8 Ga (Long et al., 2012; He et al., 2013; Zhang et al., 2013b; Ge et al., 2015). In addition, the YB and the CTB have sedimentary facies different from the Tarim Craton in the Mesoproterozoic and Paleoproterozoic (XBGMR, 1993; Li et al., 2002a). The different tectonic affinities of two blocks are also evidenced by their distinct Hf-in-zircon crustal model ages. The Hf model ages of the Tarim Craton (3.9–2.4 Ga) are distinctly older than those of the YB (3.2–1.5 Ga), implying that crustal material of the Tarim Craton formed much earlier than in the YB. Therefore, the YB and Tarim Craton most likely had different crustal histories in the Precambrian, and we therefore conclude that the YB is unlikely to have originated from the Tarim Craton.

From the above discussion, it is obvious that the Yili Block has a close tectonic relationship with the Chinese Central Tianshan Block. The Yili Block may be an exotic, isolated Precambrian block in the CAOB.

7. Conclusions

1. The meta-sediments of the lower Wenquan Group in the northern Yili Block was deposited during the early Neoproterozoic (900–845 Ma), whereas the upper was deposited at 880–857 Ma.
2. Two synchronous crustal growth and reworking events occurred in the Yili Block at ca. 1.8–1.7 and 1.6–1.3 Ga, respectively. After these events, the evolution was dominated by continuous crustal reworking from the late Mesoproterozoic to the early Neoproterozoic.
3. The Yili Block had a close tectonic affinity with the Chinese Central Tianshan Block in the Precambrian. Both terranes are unlikely to have been derived from the Siberian, North China or Tarim cratons

Supplementary data to this article can be found online at http://dx.doi.org/10.1016/j.gr.2016.05.009.

Acknowledgements

We thank Dr. Xuan-ce Wang for helpful discussions and Prof. Alfred Kröner for careful polishing on the revised version of this manuscript. The paper has benefited from review comments of two anonymous reviewers and editorial comments of Profs. Guochun Zhao and M. Santosh. This study was supported by the National Basic Research Program of China (2014CB440801) and the National Natural Science Foundation of China (41522202, 41373034, 41273012 and 41273048). This is a contribution to IGCP-Project 592 "Continental construction in Central Asia".

References

Alexeiev, D.V., Biske, Y.S., Wang, B., Djenchuraeva, A.V., Getman, O.F., Aristov, V.A., Kröner, A., Liu, H., Zhong, L., 2015. Tectono-stratigraphic framework and Palaeozoic evolution of the Chinese South Tianshan. Geotectonics 49, 93–122.

Badarch, G., Cunningham, W.D., Windley, B.F., 2002. A new terrane subdivision for Mongolia: implications for the Phanerozoic crustal growth of Central Asia. Journal of Asian Earth Sciences 21, 87–110.

Berzin, N.A., Dobretsov, N.L., 1994. Geodynamic evolution of Southern Siberia in late Precambrian–early Paleozoic time. In: Coleman, R.G. (Ed.), Reconstruction of the Paleoasian Ocean, Proc. 29th Intern Geol. Congr.VSP, Utrecht, pp. 53–70

Biske, Y.S., Seltmann, R., 2010. Paleozoic Tian–Shan as a transitional region between the Rheic and Urals–Turkestan oceans. Gondwana Research 17, 602–613.

Blichert–Toft, J., Albarede, F., 1997. The Lu–Hf geochemistry of chondrites and the evolution of the mantle–crust system. Earth and Planetary Science Letters 148, 243–258.

Buslov, M.M., Saphonova, I.Y., Watanabe, T., Obut, O.T., Fujiwara, Y., Iwata, K., Semakov, N.N., Sugai, Y., Smirnova, L.V., Kazansky, A.Y., Itaya, T., 2001. Evolution of the Paleo-Asian Ocean (Altai–Sayan, Central Asia) and Collision of Possible Gondwana-derived Terranes With the Southern Marginal Part of the Siberian Continent. Geosciences Journal 5 (3), 203–224.

Charvet, J., Shu, L.S., Laurent–Charvet, S., 2007. Paleozoic structural and geodynamic evolution of eastern Tianshan (NW China): welding of the Tarim and Junggar plates. Episodes 30, 162–186.

Charvet, J., Shu, L.S., Laurent–Charvet, S., Wang, B., Faure, M., Cluzel, D., Chen, Y., De Jong, K., 2011. Paleozoic tectonic evolution of the Tianshan belt, NW China. Science in China Series D: Earth Sciences 54 (2), 166–184.

Chen, C., Lu, H., Jia, D., Cai, D., Wu, S., 1999a. Closing history of the southern Tianshan oceanic basin, western China: an oblique collisional orogeny. Tectonophysics 302 (1–2), 23–40.

Chen, Y.B., Hu, A.Q., Zhang, G.X., 1999b. Zircon U–Pb age and Nd–Sr isotopic composition of granitic gneiss and its geological implications from Precambrian tectonic window of western Tianshan, NW China. Geochimica 28 (6), 515–520 (in Chinese with English abstract).

Chen, X.Y., Wang, Y.J., Sun, L.H., Fan, W.M., 2009. Zircon SHRIMP U–Pb dating of the granitic gneisses from Bindaban and Laerdundaban (Tianshan Orogen) and their geological significances. Geochimica 38 (5), 424–431 (in Chinese with English abstract).

Condie, K.C., 2011. Earth as an Evolving Planetary System. Elsevier, Amsterdam, Netherlands (574 p.).

Dhuime, B., Hawkesworth, C., Cawood, P., 2011. When continents formed. Science 331, 154–155.

Dobretsov, N.L., Buslov, M.M., Vernikovsky, V.A., 2003. Neoproterozoic to Early Ordovician evolution of the Paleo-Asian Ocean: implications to the breakup of Rodinia. Gondwana Research 6, 143–159.

Eizenhöfer, P.R., Zhao, G.C., Zhang, J., Sun, M., 2014. Final closure of the Paleo-Asian Ocean along the Solonker Suture Zone: constraints from geochronological and geochemical data of Permian volcanic and sedimentary rocks. Tectonics 33, 441–463.

Eizenhöfer, P.R., Zhao, G.C., Sun, M., Zhang, J., Han, Y.G., Hou, H., 2015a. Geochronological and Hf isotopic variability of detrital zircons in Palaeozoic sedimentary strata across the accretionary collision zone between the North China Craton and the Mongolian arcs, and its tectonic implications. Geological Society of America Bulletin 127, 1422–1436.

Eizenhöfer, P.R., Zhao, G.C., Zhang, J., Han, Y.G., Hou, W.Z., Liu, D.X., Wang, B., 2015b. Geochemical characteristics of the Permian basins and their provenances across the Solonker Suture Zone: assessment of net crustal growth during the closure of the Palaeo-Asian Ocean. Lithos 224–225, 240–255.

Fedo, C.M., Sircombe, K.N., Rainbird, R.H., 2003. Detrital zircon znalysis of the sedimentary record. Reviews in Mineralogy and Geochemistry 53, 277–303.

Gao, J., Li, M.S., Xiao, X.C., Tang, Y.Q., He, G.Q., 1998. Paleozoic tectonic evolution of the Tianshan Orogen, northwestern China. Tectonophysics 287, 213–231.

Gao, J., John, T., Klemd, R., Xiong, X.M., 2007. Mobilization of Ti–Nb–Ta during subduction: evidence from rutile–bearing dehydration segregations and veins hosted in eclogite, Tianshan, NW China. Geochimica et Cosmochimica Acta 71, 4974–4996.

Gao, J., Long, L.L., Klemd, R., Qian, Q., Liu, D.Y., Xiong, X.M., Su, W., Liu, W., Wang, Y.T., Yang, F.Q., 2009. Tectonic evolution of the South Tianshan orogen and adjacent regions, NW China: geochemical and a geconstraints of granitoid rocks. International Journal of Earth Sciences 98, 1221–1238.

Gao, J., Klemd, R., Qian, Q., Zhang, X., Li, J.L., Tuo, J., 2011. The collision between the Yili and Tarim blocks of the Southwestern Altaids: geochemical and age constraints of a leucogranite dike crosscutting the HPLT metamorphic belt in the Chinese Tianshan Orogen. Tectonophysics 499, 118–131. http://dx.doi.org/10.1016/j.tec to.2011.01.001.

Ge, R.F., Zhu, W.B., Wilde, S.A., Wu, H.L., He, J.W., Zheng, B.H., 2014. Archean magmatism and crustal evolution in the northern Tarim Craton: insights from zircon U–Pb–Hf–O isotopes and geochemistry of 2.7 Ga orthogneiss and amphibolite in the Korla Complex. Precambrian Research 252, 145–165.

Ge, R.F., Zhu, W.B., Wilde, S.A., He, J.W., Cui, X., 2015. Synchronous crustal growth and reworking recorded in late Paleoproterozoic granitoids in the northern Tarim craton: in situ zircon U–Pb–Hf–O isotopic and geochemical constraints and tectonic implications. Geological Society of America Bulletin 127, 781–803.

Gehrels, G., 2014. Detrital zircon U–Pb geochronology applied to tectonics. Annual Review of Earth and Planetary Sciences 42, 127–149.

Gladkochub, D., Donskaya, T., 2009. Overview of geology and tectonic evolution of the Baikal–Tuva area. In: Müller, W.E.G., Grachev, M.A. (Eds.), Biosilica in Evolution, Morphogenesis, and Nanobiotechnology. Springer–Verlag, Berlin–Heidelberg, pp. 3–26.

Gladkochub, D., Pisarevsky, S., Donskaya, T., Natapov, L., Mazukabzov, A., Stanevich, A., Sklyarov, E., 2006. The Siberian Craton and its evolution in terms of the Rodinia hypothesis. Episodes 29, 169–174.

Glorie, S., De Grave, J., Buslov, M.M., Zhimulev, F.I., Safonova, I.Y., 2014. Detrital zircon provenance of early Palaeozoic sediments at the southwestern margin of the Siberian Craton: insights from U–Pb geochronology. Journal of Asian Earth Sciences 82, 115–123.

Greentree, M.R., Li, Z.X., Li, X.H., Wu, H., 2006. Late Mesoproterozoic to earliest Neoproterozoic basin record of the Sibao orogenesis in western South China and relationship to the assembly of Rodinia. Precambrian Research 151, 79–100.

Griffin, W.L., Wang, X., Jackson, S.E., Pearson, N.J., O'Reilly, S.Y., Xu, X., Zhou, X., 2002. Zircon chemistry and magma mixing, SE China: in-situ analysis of Hf isotopes. Tonglu and Pingtan igneous complexes. Lithos 61, 237–269.

Griffin, W.L., Belousova, E.A., Shee, S.R., Pearson, N.J., O'Reily, S.Y., 2004. Archean crustal evolution in the northern Yilgarn Craton: U–Pb and Hf-isotope evidence from detrital zircons. Precambrian Research 13l, 23l–282.

Han, B.F., Guo, Z.J., Zhang, Z.C., Zhang, L., Chen, J.F., Song, B., 2010. Age, geochemistry, and tectonic implications of a late Paleozoic stitching pluton in the North Tian Shan suture zone, western China. Geological Society of America Bulletin 122, 627–640.

Han, Y.G., Zhao, G.C., Sun, M., Eizenhöfer, P.R., Hou, W.Z., Zhang, X.R., Liu, D.X., Wang, B., Zhang, G.W., 2015. Paleozoic accretionary orogenesis in the Paleo-Asian Ocean: insights from detrital zircons from Silurian to Carboniferous strata at the northwestern margin of the Tarim Craton. Tectonics 34, 334–351.

Han, Y.G., Zhao, G.C., Sun, M., Eizenhöfer, P.R., Hou, W.Z., Zhang, X.R., Liu, Q., Wang, B., Liu, D.X., Xu, B., 2016a. Late Paleozoic subduction and collision processes during the amalgamation of the Central Asian Orogenic Belt along the South Tianshan suture zone. Lithos 246–247, 1–12.

Han, Y.G., Zhao, G.C., Cawood, P.A., Sun, M., Eizenhöfer, P.R., Hou, W.Z., Zhang, X.R., Liu, Q., 2016b. Tarim and North China cratons linked to northern Gondwana through switching accretionary tectonics and collisional orogenesis. Geology 44, 95–98.

He, Z.Y., Zhang, Z.M., Zong, K.Q., Wang, W., Yu, F., 2012. Zircon geochronology of Xingxingxia quartz dioritic gneisses: implications for the tectonic evolution and Precambrian basement affinity of Chinese Tianshan orogenic belt. Acta Petrologica Sinica 28 (6), 1857–1874 (in Chinese with English abstract).

He, Z.Y., Zhang, Z.M., Zong, K.Q., Dong, X., 2013. Paleoproterozoic crustal evolution of the Tarim Craton: constrained by zircon U–Pb and Hf isotopes of meta-igneous rocks from Korla and Dunhuang. Journal of Asian Earth Sciences 78, 54–70.

He, J.W., Zhu, W.B., Ge, R.F., 2014a. New age constraints on Neoproterozoic diamicites in Kuruktag, NW China and Precambrian crustal evolution of the Tarim Craton. Precambrian Research 241, 44–60.

He, J.W., Zhu, W.B., Ge, R.F., Zheng, B.H., Wu, H.L., 2014b. Detrital zircon U–Pb ages and Hf isotopes of Neoproterozoic strata in the Aksu area, northwestern Tarim Craton: implications for supercontinent reconstruction and crustal evolution. Precambrian Research 254, 194–209.

He, Z.Y., Zhang, Z.M., Zong, K.Q., Xiang, H., Chen, X.J., Xia, M.J., 2014c. Zircon U–Pb and Hf isotopic studies of the Xingxingxia Complex from Eastern Tianshan (NW China): significance to the reconstruction and tectonics of the southern Central Asian Orogenic Belt. Lithos 190–191, 485–499.

He, J.W., Zhu, W.B., Zheng, B.H., Wu, H.L., Cui, X., Lu, Y.Z., 2015. Neoproterozoic diamictite-bearing sedimentary rocks in the northern Yili Block and their constraints on the Precambrian evolution of microcontinents in the Western Central Asian Orogenic Belt. Tectonophysics 665, 23–36.

Hoskin, P.W.O., Schaltegger, U., 2003. The composition of zircon and igneous and metamorphic petrogenesis. Reviews in Mineralogy and Geochemistry 53, 27–62.

Hu, A.Q., Jahn, B.M., Zhang, G.X., Zhang, Q.F., 2000. Crustal evolution and Phanerozoic crustal growth in northern Xinjiang: Nd–Sr isotopic evidence. Tectonophysics 328, 15–51.

Hu, A.Q., Wei, G.J., Zhang, J.B., Deng, W.F., Chen, L.L., 2008. SHRIMP U–Pb ages for zircons of the amphibolites and tectonic evolution significance from the Wenquan domain in the West Tianshan Mountains, Xinjiang, China. Acta Petrologica Sinica 24 (12), 2731–2740 (in Chinese with English abstract).

Hu, A.Q., Wei, G.J., Jahn, B.M., Zhang, J.B., Deng, W.F., Chen, L.L., 2010. Formation of the 0.9 Ga Neoproterozoic granitoids in the Tianshan Orogen, NW China: constraints from the SHRIMP zircon age determination and its tectonic significance. Geochimica 39 (3), 197–212 (in Chinese with English abstract).

Huang, Z.Y., Long, X.P., Kröner, A., Yuan, C., Wang, Q., Sun, M., Zhao, G.C., Wang, Y.J., 2013. Geochemistry, zircon U–Pb ages and Lu–Hf isotopes of early Paleozoic plutons in the northwestern Chinese Tianshan: petrogenesis and geological implications. Lithos 182–183, 48–66.

Huang, B.T., He, Z.Y., Zong, K.Q., Zhang, Z.M., 2014. Zircon U–Pb and Hf isotopic study of Neopeoterozoic granitic gneisses from the Alatage area, Xingjiang: constraints on the Precambrian crustal evolution in the Central Tianshan Block. Chinese Science Bulletin 59 (1), 100–112 (in Chinese with English abstract).

Huang, B.T., He, Z.Y., Zhang, Z.M., Klemd, R., Zong, K.Q., Zhao, Z.D., 2015a. Early Neoproterozoic granitic gneisses in the Chinese Eastern Tianshan: petrogenesis and tectonic implications. Journal of Asian Earth Sciences 113, 339–352.

Huang, Z.Y., Long, X.P., Kröner, A., Yuan, C., Wang, Y.J., Chen, B., Zhang, Y.Y., 2015b. Neoproterozoic granitic gneisses in the Chinese Central Tianshan Block: implications for tectonic affinity and Precambrian crustal evolution. Precambrian Research 269, 73–89.

Jahn, B.M., Wu, F.Y., Chen, B., 2000. Massive granitoid generation in Central Asia: Nd isotope evidence and implication for continental growth in the Phanerozoic. Episodes 23, 82–92.

Jahn, B.M., Windley, B., Natal'in, B., Dobretsov, N., 2004. Phanerozoic continental growth in Central Asia. Journal of Asian Earth Sciences 23, 599–603.

Kheraskova, T.N., Didenko, A.N., Bush, V.A., Volozh, Y.A., 2003. The Vendian–Early Paleozoic history of the continental margin of eastern Paleogondwana, Paleoasian Ocean, and Central Asian Foldbelt. Russian Journal of Earth Sciences 5 (3), 165–184.

Khudoley, A.K., Rainbird, R.H., Stern, R.A., Kropachev, A.P., Heaman, L.M., Zanin, A.M., Podkovyrov, V.N., Belova, V.N., Sukhorukov, V.I., 2001. Sedimentary evolution of the Riphean–Vendian basin of southeastern Siberia. Precambrian Research 129–163.

Klemd, R., Brocker, M., Hacker, B.R., 2005. New age constraints on the metamorphic evolution of the high-pressure/low-temperature belt in the western Tianshan Mountains, NW China. The Journal of Geology 113, 157–168.

Klemd, R., John, T., Scherer, E., Rondenay, S., Gao, J., 2011. Changes in dip of subducted slabs at depth: petrological and geochronological evidence from HP–UHP rocks (Tianshan, NW-China). Earth and Planetary Science Letters 310, 9–20.

Klemd, R., Gao, J., Li, J.L., Meyer, M., 2015. Metamorphic evolution of (ultra)-high-pressure subduction-related transient crust in the South Tianshan Orogen (Central Asian Orogenic Belt): geodynamic implications. Gondwana Research 28, 1–25.

Kröner, A., Alexeiev, D.V., Hegner, E., Rojas–Agramonte, Y., Corsini, M., Chao, Y., Wong, J., Windley, B.F., Liu, D., Tretyakov, A.A., 2012. Zircon and muscovite ages, geochemistry, and Nd–Hf isotopes for the Aktyuz metamorphic terrane: evidence for an Early Ordovician collisional belt in the northern Tianshan of Kyrgyzstan. Gondwana Research 21, 901–927.

Kröner, A., Alexeiev, D.V., Rojas–Agramonte, Y., Hegner, E., Wong, J., Xia, X., Belousova, E., Mikolaichuk, A.V., Seltmann, R., Liu, D., Kiselev, V.V., 2013. Mesoproterozoic (Grenville–age) terranes in the Kyrgyz North Tianshan: zircon ages and Nd–Hf isotopic constraints on the origin and evolution of basement blocks in the southern Central Asian Orogen. Gondwana Research 23, 272–295.

Kuzmichev, A.B., Bibikova, E.V., Zhuravlev, D.Z., 2001. Neoproterozoic (~800 Ma) orogeny in the Tuva–Mongol massif (Siberia): island arc–continent collision at the northeast Rodinia margin. Precambrian Research 110 (1–4), 109–126.

Laurent–Charvet, S., Monié, P., Shu, L.S., 2003. Late Paleozoic strike–slip shear zones in eastern Central Asia (NW China): new structural and geochronological data. Tectonics 22 (2), 24.

Lei, R.X., Wu, C.Z., Gu, L.X., Zhang, Z.Z., Chi, G.X., Jiang, Y.H., 2011. Zircon U–Pb chronology and Hf isotope of the Xingxingxia granodiorite from the Central Tianshan zone (NW China): implications for the tectonic evolution of the southern Altaids. Gondwana Research 20, 582–593.

Lei, R.X., Wu, C.Z., Chi, G.X., Chen, G., Gu, L.X., Jiang, Y.H., 2012. Petrogenesis of the Palaeoproterozoic Xishankou pluton, northern Tarim block, northwest China: implications for assembly of the supercontinent Columbia. International Geology Review 54, 1829–1842.

Lei, R.X., Wu, C.Z., Chi, G.X., Gu, L.X., Zhong, L.H., Qu, X., Jiang, Y.H., Jiang, S.Y., 2013. The Neoproterozoic Hongliujing A-type granite in Central Tianshan (NW China): LA-ICP-MS zircon U–Pb geochronology, geochemistry Nd–Hf isotope and tectonic significance. Journal of Asian Earth Sciences 74, 142–154.

Levashova, N.M., Van der Voo, R., Abrajevitch, A.V., Bazhenov, M.L., 2009. Paleomagnetism of mid-Paleozoic subduction-related volcanics from the Chingiz Range in NE Kazakhstan: the evolving paleogeography of the amalgamating Eurasian composite continent. Geological Society of America Bulletin 121, 555–573.

Levashova, N.M., Meert, J.G., Gibsher, A.S., Grice, W.C., Bazhenov, M.L., 2011. The origin of microcontinents in the Central Asian Orogenic Belt: constraints from paleomagnetism and geochronology. Precambrian Research 185, 37–54.

Li, Q., Yu, H.F., Xiu, Q.F., 2002a. On precambrian basement of the eastern Tianshan mountain, Xinjiang. Xinjiang Geology 20, 346–351 (in Chinese with English abstract).

Li, Z.X., Li, X.H., Zhou, H.W., Kinny, P.D., 2002b. Grenvillian continental collision in south China: new SHRIMP U–Pb zircon results and implic ations for the con figuration of Rodinia. Geology 30, 163–166.

Li, Q.G., Liu, S.W., Wang, Z.Q., Yan, Q.R., Guo, Z.J., Zhang, Z.C., Zheng, H.F., Jiang, C.F., Wang, T., Chu, Z.Y., 2007. Geochemical constraints on the petrogenesis of the Proterozic granitoid gneisses from the eastern segment of the Central Tianshan Tectonic Zone, northwestern China. Geological Magazine 144 (2), 305–317.

Li, Z.X., Bogdanova, S.V., Collins, A.S., Davidson, A., De Waele, B., Ernst, R.E., Fitzsi–mons, I.C.W., Fuck, R.A., Gladkochub, D.P., Jacobs, J., Karlstrom, K.E., Natapovm, L.M., Lu, S., Natapov, L.M., Pease, V., Pisarevsky, S.A., Thrane, K., Vernikovsky, V., 2008. Assembly, configuration, and break-up history of Rodinia: a synthesis. Precambrian Research 160, 179–210.

Li, J.L., Su, W., Zhang, X., Liu, X., 2009. Zircon Cameca U–Pb dating and its significance for granulite–facies gneisses from the western Awulale Mountain, Western Tianshan, China. Geological Bulletin of China 28 (12), 1852–1862 (in Chinese with English abstract).

Li, H., Zhang, H., Ling, M.X., Wang, F.Y., Ding, X., Zhou, J.B., Yang, X.Y., Tu, X.L., Sun, W.D., 2011. Geochemical and zircon U–Pb study of the Huangmeijian A-type granite: implications for geological evolution of the Lower Yangtze River belt. International Geology Review 53, 499–525.

Li, K.S., Wang, B., Shu, L.S., Wang, F., Liu, H.S., 2013. Geological features, ages, and tectonic implications of the Wenquan Group in NW Chinese Tianshan. Geochemical Journal of China University 19, 491–503 (in Chinese with English abstract).

Li, X.H., Li, Z.X., Li, W.X., 2014. Detrital zircon U–Pb age and Hf isotope constrains on the generation and reworking of Precambrian continental crust in the Cathaysia Block, South China: a synthesis. Gondwana Research 25, 1202–1215.

Liu, S.W., Guo, Z.J., Zhang, Z.C., 2004. Nature of the Precambrian metamorphic blocks in the eastern segment of Central Tianshan: constraints from geochronology and Nd isotopic geo-chemistry. Science in China Series D: Earth Sciences 47, 1085–1094 (in Chinese with English abstract).

Liu, H.S., Wang, B., Shu, L.S., Jahn, B.M., Lizuka, Y., Chen, Y., 2014. Detrital zircon ages of Proterozoic meta-sedimentary rocks and Paleozoic sedimentary cover of the northern Yili Block: implications for the tectonics of microcontinents in the Central Asian Orogenic Belt. Precambrian Research 252, 209–222.

Long, X.P., Yuan, C., Sun, M., Zhao, G.C., Xiao, W.J., Wang, W.J., Yang, Y.H., Hu, A.Q., 2010. Archean crustal evolution of the northern Tarim craton, NW China: zircon U–Pb and Hf isotopic constraints. Precambrian Research 180, 272–284.

Long, L.L., Gao, J., Klemd, R., Beier, C., Qian, Q., Zhang, X., Wang, J.B., Jiang, T., 2011a. Geochemical and geochronological studies of granitoid rocks from the Western Tianshan Orogen: implications for continental growth in the southwestern Central Asian Orogenic Belt. Lithos 126, 321–340.

Long, X.P., Yuan, C., Sun, M., Kröner, A., Zhao, G.C., Wilde, S., Hu, A.Q., 2011b. Reworking of the northern Tarim Craton by underplating of mantle plume–derived magmas: evidence from Neoproterozoic adakitic rocks in the Kuluketage area, NW China. Precambrian Research 187, 1–14.

Long, X.P., Yuan, C., Sun, M., Xiao, W.J., Zhao, G.C., Zhou, K.F., Wang, Y.J., Hu, A.Q., 2011c. The discovery of the oldest rocks in the Kuluketage area and its geological implications. Science China Earth Sciences 54 (3), 342–348.

Long, X.P., Sun, M., Yuan, C., Kröner, A., Hu, A., 2012. Zircon REE patterns and geochemical characteristics of Paleoproterozoic anatectic granite in the northern Tarim Craton, NW China: implications for the reconstruction of the Columbia supercontinent. Precambrian Research 222–223, 474–487.

Ludwig, K.R., 2003. User's manual for Isoplot 3.00: a geochronological toolkit for Microsoft Excel. Special Publication. 4a. Berkeley Geochronol. Cent, Berkeley, Calif.

Luo, Y., Sun, M., Zhao, G.C., Li, S.Z., Ayers, J.C., Xia, X.P., Zhang, J.H., 2008. A comparison of U–Pb and Hf isotopic compositions of detrital zircons from the North and South Liaohe Groups: constraints on the evolution of the Jiao–Liao–Ji Belt, North China Craton. Precambrian Research 163, 279–306.

Ma, X.X., Shu, L., Jahn, B.M., Zhu, W., Faure, M., 2012a. Precambrian tectonic evolution of Central Tianshan, NW China: constraints from U–Pb dating and in situ Hf isotopic analysis of detrital zircons. Precambrian Research 222–223, 450–473.

Ma, X.X., Shu, L., Santosh, M., Li, J., 2012b. Detrital zircon U–Pb geochronology and Hf isotope data from Central Tianshan suggesting a link with the Tarim Block: implications on Proterozoic supercontinent history. Precambrian Research 206–207, 1–16.

Ma, X.X., Shu, L.L., Santosh, M., Li, J.Y., 2013. Paleoproterozoic collisional orogeny in Central Tianshan: assembling the Tarim Block within the Columbia supercontinent. Precambrian Research 228, 1–19.

Machado, N., Simonetti, A., 2001. U–Pb dating and hf isotopic composition of zircon by laser ablation-MC-ICP-MS. Laser Ablation-ICPMS in the Earth Sciences. Mineralogical Association of Canada Short Course vol. 29, pp. 121–146.

Metcalfe, I., 2013. Gondwana dispersion and Asian accretion: tectonic and palaeogeographic evolution of eastern Tethys. Journal of Asian Earth Sciences 66, 1–33.

Nelson, D.R., 2001. An assessment of the determination of depositional ages for Precambrian clastic sedimentary rocks by U–Pb dating of detrital zircons. Sedimentary Geology 141–142, 37–60.

Peng, P., Zhai, M.G., Guo, J.H., Kusky, T., Zhao, T.P., 2007. Nature of mantle source contributions and crystal differentiation in the petrogenesis of the 1.78 Ga mafic dykes in the central North China craton. Gondwana Research 12, 29–46.

Peng, P., Zhai, M.G., Ernst, R.E., Guo, J.H., Liu, F., Hu, B., 2008. A 1.78 Ga large igneous province in the North China craton: the Xiong'er Volcanic Province and the North China dyke swarm. Lithos 101, 260–280.

Poller, U., Gladkochub, D., Donskaya, T., Mazukabzow, A., Sklyarov, E., Todt, W., 2005. Multistage magmatic and metamorphic evolution in the Southern Siberian Craton: Archean and Paleoproterozoic zircon ages revealed by SHRIMP and TIMS. Precambrian Research 136 (2531–368).

Powerman, V., Shatsillo, A., Chumakov, N., Kapitonov, I., Hourigan, J., 2015. Interaction between the Central Asian Orogenic Belt (CAOB) and the Siberian craton as recorded by detrital zircon suites from Transbaikalia. Precambrian Research 267, 39–71.

Qian, Q., Gao, J., Klemd, R., He, G.Q., Xiong, X.M., Long, L.L., Liu, D.Y., Xu, R.H., 2009. Early Paleozoic tectonic evolution of the Chinese South Tianshan Orogen: constraints from SHRIMP zircon U–Pb geochronology and geochemistry of basaltic and dioritic rocks from Xiate, NW China. International Journal of Earth Sciences 98, 551–569.

Qiu, X.F., Ling, W.L., Liu, X.M., Kusky, T., Berkana, W., Zhang, Y.H., Gao, Y.J., Lu, S.S., Kuang, H., Liu, C.X., 2011. Recognition of Grenvillian volcanic suite in the Shennongjia region and its tectonic significance for the South China Craton. Precambrian Research 191, 101–119.

Rojas-Agramonte, Y., Kröner, A., Alexeiev, D.V., Jeffreys, T., Khudoley, A.K., Wong, J., Geng, H., Shu, L., Semiletkin, S.A., Mikolaichuk, A.V., Kiselev, V.V., Yang, J., Seltmann, R., 2014. Detrital and igneous zircon ages for supracrustal rocks of the Kyrgyz Tianshan and palaeogeographic implications. Gondwana Research 26, 957–974.

Rojas–Agramonte, Y., Kröner, A., Demoux, A., Xia, X., Wang, W., Donskaya, T., Liu, D., Sun, M., 2011. Detrital and xenocrystic zircon ages from Neoproterozoic to Palaeozoic arc terranes of Mongolia: significance for the origin of crustal fragments in the Central Asian Orogenic Belt. Gondwana Research 19, 751–763.

Rosen, O.M., Condie, K.C., Natapov, L.M., Nozhkin, A.D., 1994. Archean and early Proterozoic evolution of the Siberian craton: a preliminary assessment. In: Condie, K.C. (Ed.), Archean Crustal Evolution. Elsevier, Amsterdam, pp. 411–459.

Sengör, A.M.C., Natal'in, B.A., 1996. Paleotectonics of Asia: fragments of a synthesis. In: Yin, A., et al. (Eds.), The Tectonic Evolution of Asia. Cambridge University Press, Cambridge, pp. 486–640.

Shu, L.S., Yu, J.H., Charvet, J., Laurent–Charvet, S., Sang, H.Q., Zhang, R.G., 2004. Geological, geochronological and geochemical features of granulites in the Eastern Tianshan, NW China. Journal of Asian Earth Sciences 24, 25–41.

Shu, L.S., Deng, X.L., Zhu, W.B., Ma, D.S., Xiao, W.J., 2011. Precambrian tectonic evolution of the Tarim Block, NW China: new geochronological insights from the Quruqtagh domain. Journal of Asian Earth Sciences 42 (5), 774–790.

Shu, L.S., Zhu, W.B., Wang, B., Wu, C.Z., Ma, D.Y., Ma, X.X., Ding, H.F., 2013. The formation and evolution of ancient blocks in Xinjiang. Geology in China 40 (1), 43–60 (in Chinese with English abstract).

Söderlund, U., Patchett, P.J., Vervoort, J.D., Isachsen, C.E., 2004. The 176Lu decay constant determined by Lu–Hf and U–Pb isotope systematics of Precambrian mafic intrusions. Earth and Planetary Science Letters 219 (3–4), 311–324.

Tang, G.J., Wang, Q., Wyman, D.A., Sun, M., Li, Z.X., Zhao, Z.H., Sun, W.D., Jia, X.H., Jiang, Z.Q., 2010. Geochronology and geochemistry of Late Paleozoic magmatic rocks in the Lamasu–Dabate area, northwestern Tianshan (west China): evidence for a tectonic transition from arc to post-collisional setting. Lithos 393–411.

Taylor, S.R., McLennan, S., 2009. Planetary Crusts: Their Composition, Origin and Evolution. Cambridge University Press, Cambridge, UK (378 p.).

Turkina, O.M., Nozhkin, A.D., Bayanova, T.B., Dmitrieva, N.V., Travin, A.V., 2007. Precambrian terranes in the southwestern framing of the Siberian craton: isotopic provinces, stages of crustal evolution and accretion–collision events. Russian Geology and Geophysics 48 (1), 61–70.

Wan, Y.S., Liu, D.Y., Song, B., 2005. Geochemical and Nd isotopic composition of 3.8 Ga meta-quartz dioritic and trondhjemitic rocks from the Archean area and their geological significance. Journal of Asian Earth Sciences 24, 563–575.

Wan, Y.S., Song, B., Liu, D.Y., Wilde, S.A., Wu, J.S., Shi, Y.R., Yin, X.Y., Zhou, H.Y., 2006. SHRIMP U–Pb zircon geochronology of Palaeoproterozoic metasedimentary rocks in the North China Craton: evidence for a major Late Palaeoproterozoic tectonothermal event. Precambrian Research 149, 249–271.

Wang, B., Faure, M., Cluzel, D., Shu, L.S., Charvet, J., Meffre, S., Ma, Q., 2006. Late Paleozoic tectonic evolution of the northern West Chinese Tianshan Belt. Geodinamica Acta 19, 237–247.

Wang, Q., Wyman, D.A., Zhao, Z.H., Xu, J.F., Bai, Z.H., Xiong, X.L., Dai, T.M., Li, C.F., Chu, Z.Y., 2007. Petrogenesis of Carboniferous adakites and Nb enriched arc basalts in the Alataw area, northern Tianshan Range (western China): implications for Phanerozoic crustal growth in the Central Asia orogenic belt. Chemical Geology 236, 42–64.

Wang, B., Faure, M., Shu, L.S., Cluzel, D., Charvet, J., Jong, K.D., Chen, Y., 2008. Paleozoic tectonic evolution of the Yili Block, western Chinese Tianshan. Bulletin de la Societe Geologique de France 179 (5), 483–490.

Wang, B., Jahn, B.M., Shu, L.S., Li, K.S., Chung, S.L., Liu, D.Y., 2012. Middle–Late Ordovician arc-type plutonism in the NW Chinese Tianshan: implication for the accretion of the Kazakhstan continent in Central Asia. Journal of Asian Earth Sciences 49, 40–53.

Wang, B., Liu, H.S., Shu, L.S., Jahn, B.M., Chung, S.L., Zhai, Y.Z., Liu, D.Y., 2014a. Early Neoproterozoic crustal evolution in northern Yili Block: insights for mmigmatite, orthogneiss and leucogranite of the Wenquan metamorphic complex in the NW Chinese Tianshan. Precambrian Research 242, 58–81.

Wang, B., Shu, L.S., Liu, H.S., Gong, H.J., Ma, Y.Z., Mu, L.X., Zhong, L.L., 2014b. First evidence for ca. 780 Ma intra-plate magmatism and its implications for Neoproterozoic rift of the North Yili Block and tectonic origin of the continental blokcs in SW of Central Asia. Precambrian Research 254, 258–272.

Wang, Z.M., Han, C.M., Xiao, W.J., Su, B.X., Sakyi, P.A., Song, D.F., Lin, L.N., 2014c. The petrogenesis and tectonic implications of the granitoid gneisses from Xingxingxia in the eastern segment of Central Tianshan. Journal of Asian Earth Sciences 88, 277–292.

Windley, B.F., Alexeiev, D., Xiao, W., Kröner, A., Badarch, G., 2007. Tectonic models for accretion of the Central Asian Orogenic Belt. Journal of the Geological Society 164, 31–47.

Wu, Y.B., Zheng, Y.F., 2004. Genesis of zircon and its constraints on interpretation of U–Pb age. Chinese Science Bulletin 49, 1554–1569 (in Chinese with English abstract).

Wu, F.Y., Yang, Y.H., Xie, L.W., Yang, J.H., Xu, P., 2006. Hf isotopic compositions of the standard zircons and baddeleyites used in U–Pb geochronology. Chemical Geology 234, 105–126.

Wu, F.Y., Zhang, Y.B., Yang, J.H., Xie, L.W., Yang, Y.H., 2008. Zircon U–Pb and Hf isotopic constraints on the Early Archean crustal evolution in Anshan of the North China Craton. Precambrian Research 167, 339–362.

Wu, C.Z., Santosh, M., Chen, Y.J., Samson, I.M., Lei, R.X., Dong, L.H., Qu, X., Gu, L.X., 2014. Geochronology and geochemistry of Early Mesoproterozoic meta-diabase sills from Quruqtagh in the northeastern Tarim Craton: implications for breakup of the Columbia supercontinent. Precambrian Research 241, 29–43.

XBGMR (Xinjiang Bureau of Geology and Mineral Resources), 1993,. Regional Geology of Xinjiang Uygur Autonomy Region. Geology Publishing House, Beijing, pp. 1–841.

Xia, X.P., Sun, M., Zhao, G.C., Luo, Y., 2006a. LA-ICP-MS U–Pb geochronology of detrital zircons from the Jining Complex, North China Craton and its tectonic significance. Precambrian Research 144, 199–212.

Xia, X.P., Sun, M., Zhao, G.C., Wu, F., Xu, P., Zhang, J.H., Luo, Y., 2006b. U–Pb and Hf isotopic study of detrital zircons from the Wulashan khondalites: constraints on the evolution of the Ordos Terrane, Western Block of the North China Craton. Earth and Planetary Science Letters 241, 581–593.

Xiao, W.J., Windley, B.F., Badararch, G., Sun, S., Li, J., Qin, K., Wang, Z., 2004. Paleozoic accretionary and convergent tectonics of the southern Altaids: implications for the growth of Central Asia. Journal of the Geological Society of London 161, 1–4.

Xiao, W.J., Han, C.M., Yuan, C., Sun, M., Lind, S., Chen, H.L., Li, Z.L., Sun, S., 2008. Middle Cambrian to Permian subduction-related accretionary orogenesis of Northern Xinjiang, NW China: implications for the tectonic evolution of central Asia. Journal of Asian Earth Sciences 32, 102–117.

Xiao, W.J., Huang, B.C., Han, C.M., Sun, S., Li, J.L., 2010. A review of the western part of the Altaids: a key to understanding the architecture of accretionary orogens. Gondwana Research 18, 253–273.

Xiao, W.J., Windley, B.F., Allen, M.B., Han, C.M., 2013. Paleozoic multiple accretionary and collisional tectonics of the Chinese Tianshan orogenic collage. Gondwana Research 23, 1316–1341.

Xiong, Q., Zheng, J.P., Yu, C.M., Su, Y.P., Tang, H.Y., Zhang, Z.H., 2009. Zircon U–Pb age and Hf isotope of Quanyishang A-type granite in Yichang: signification for the Yangtze continental cratonization in Paleoproterozoic. Chinese Science Bulletin 54, 436–446.

Xu, X.Y., Ma, Z.P., Xia, L.Q., Wang, Y.B., Li, X.M., Xia, Z.C., Wang, L.S., 2005. SHRIMP dating of plagiogranites from Bayingou ophiolite in the northern Tianshan Mountains. Geological Review 22 (5), 523–527 (in Chinese with English abstract).

Xu, Z.Q., He, B.Z., Zhang, C.L., Zhang, J.X., Wang, Z.M., Cai, Z.H., 2013. Tectonic framework and crustal evolution of the Precambrian basement of the Tarim Block in NW China: new geochronological evidence from deep drilling samples. Precambrian Research 235, 150–162.

Zhai, M.G., 2004. Precambrian tectonic evolution of the North China Craton. In: Malpas, J., Fletcher, C.J.N., Ali, J.R., Aitchison, J.C. (Eds.), Aspects of the Tectonic Evolution of China. Geological Society Special Publications Vol. 226, pp. 57–72.

Zhang, L.F., Ellis, D.J., Williams, S., 2003. Ultrahigh pressure metamorphism in eclogites from the Western Tianshan, China — reply. American Mineralogist 88, 1157–1160.

Zhang, D.Y., Zhang, Z.C., Encarnación, J., Xue, C.J., Duan, S.G., Zhao, Z.D., Liu, J.L., 2012a. Petrogenesis of the Kekesai composite intrusion, western Tianshan, NW China: implications for tectonic evolution during late Paleozoic time. Lithos 146–147, 65–79. http://dx.doi.org/10.1016/j.lithos.2012.04.002.

Zhang, C.L., Zou, H.B., Wang, H.Y., Li, H.K., Ye, H.M., 2012b. Multiple phases of the Neoproterozoic igneous activity in Quruqtagh of the northeastern Tarim Block, NW China: interaction between plate subduction and mantle plume? Precambrian Research 222–223, 488–502.

Zhang, S.H., Zhao, Y., Santosh, M., 2012c. Mid-Mesoproterozoic bimodal magmatic rocks in the northern North China Craton: implications for magmatism related to breakup of the Columbia supercontinent. Precambrian Research 222–223, 339–367.

Zhang, C.L., Zou, H.B., Li, H.K., 2013a. Tectonic framework and evolution of the Tarim Block, NW China. Gondwana Research 23, 1306–1315.

Zhang, J., Yu, S., Gong, J., Li, H., Hou, K., 2013b. The latest Neoarchean–Paleoproterozoic evolution of the Dunhuang block, eastern Tarim craton, northwestern China: evidence from zircon U–Pb dating and Hf isotopic analyses. Precambrian Research 226, 21–42.

Zhang, X.R., Zhao, G.C., Eizenhöfer, P.R., Sun, M., Han, Y.G., Hou, W.Z., Liu, D.X., Wang, B., Liu, Q., Xu, B., 2015a. Latest Carboniferous closure of the Junggar Ocean constrained by geochemical and zircon U–Pb–Hf isotopic data of granitic gneisses from the Central Tianshan block, NW China. Lithos 238, 26–36.

Zhang, X.R., Zhao, G.C., Eizenhöfer, P.R., Sun, M., Han, Y.G., Hou, W.Z., Liu, D.X., Wang, B., Liu, Q., Xu, B., 2015b. Paleozoic magmatism and metamorphism in the Central Tianshan block revealed by U–Pb and Lu-Hf isotope studies of detrital zircons from the South Tianshan belt, NW China. Lithos 233, 193–208.

Zhang, J., Sun, M., Schulmann, K., Zhao, G.C., Wu, Q., Jiang, Y.D., Guy, A., Wang, Y.J., 2015c. Distinct deformational history of two contrasting tectonic domains in the Chinese Altai: their significance in understanding accretionary orogenic process. Journal of Structural Geology 73, 64–82.

Zhang, X.R., Zhao, G.C., Sun, M., Eizenhöfer, P.R., Han, Y.G., Hou, W.Z., Liu, D.X., Wang, B., Zhu, Y.L., Liu, Q., Xu, B., 2016. Tectonic evolution from oceanic subduction to arc–continent collision of the Junggar Ocean: constraints from U–Pb dating and Hf isotopes of detrital zircons from the North Tianshan belt, NW China. Geological Society of America Bulletin http://dx.doi.org/10.1130/B31230.1.

Zhao, G.C., 2009. Metamorphic evolution of major tectonic units in the basement of the North China Craton: key issues and discussion. Acta Petrologica Sinica 25, 1772–1792 (in Chinese with English abstract).

Zhao, G.C., Wilde, S.A., Guo, J.H., Cawood, P.A., Sun, M., Li, X.P., 2010. Single zircon grains record two continental collisional events in the North China craton. Precambrian Research 177, 266–276.

Zhao, P., Chen, Y., Zhan, S., Xu, B., Faure, M., 2014. The apparent polar wander path of the Tarim block (NW China) since the Neoproterozoic and its implications for a long-term Tarim–Australia connection. Precambrian Research 242, 39–57.

Zhou, J.B., Wilde, S.A., Zhang, X.Z., Zhao, G.C., Zheng, C.Q., Wang, Y.J., Zhang, X.H., 2009. The onset of Pacific margin accretion in NE China: evidence from the Heilongjiang high-pressure metamorphic belt. Tectonophysics 478, 230–246.

Zhou, J.B., Wilde, S.A., Zhao, G.C., Zhang, X.Z., Zheng, C.Q., Wang, H., 2010a. Pan-African metamorphic and magmatic rocks of the Khanka Massif, NE China: further evidence regarding their affinity. Geological Magazine 147, 737–749.

Zhou, J.B., Wilde, S.A., Zhao, G.C., Zhang, X.Z., Zheng, C.Q., Wang, H., 2010b. New SHRIMP U–Pb zircon ages from the Heilongjiang high-pressure belt: constraints on the Mesozoic evolution of NE China. American Journal of Science 310, 1024–1053.

Zhou, J.B., Wilde, S.A., Zhao, G.C., Zhang, X.Z., Zheng, C.Q., Wang, H., Zeng, W.S., 2010c. An intriguing dilemma: was the easternmost segment of the Central Asian Orogenic Belt derived from Gondwana. Journal of Geodynamics 50, 300–317.

Zhou, J.B., Wilde, S.A., Zhang, X.Z., Zhao, G.C., Liu, F.L., Qiao, D.W., Ren, S.M., Liu, J.H., 2011. A >1300 km late Pan-African metamorphic belt in NE China: new evidence from the Xing'an block and its tectonic implications. Tectonophysics 509, 280–292.

Zhu, W.B., Zheng, B.H., Shu, L.S., Ma, D.S., Wu, H.L., Li, Y.X., Huang, W.T., Yu, J.J., 2011. Neoproterozoic tectonic evolution of the Precambrian Aksu blueschist terrane, northwestern Tarim, China: insights from LA-ICP-MS zircon U–Pb ages and geochemical data. Precambrian Research 185, 215–230.

Zhu, Z.X., Dong, L.H., Wang, K.Z., Zhao, T.Y., Xu, S.Q., Chen, B.X., Li, P., Jin, L.Y., 2013. Tectonic division and regional tectonic evolution of West Tianshan belt. Geological Bulletin of China 32, 297–306 (In Chinese with English abstract).

Zonenshain, L.P., Kuzmin, M.I., Natapov, L.M., 1990. Geology of the USSR: a platetectonic synthesis. Geodynamics Series 21. American Geophysical Union, Washington, D.C, p. 242.